Physiological Roles of GRASP55 in Lipid Transport

Jiyoon Kim
Department of Medical Science
The Graduate School, Yonsei University

Physiological Roles of GRASP55 in Lipid Transport

Jiyoon Kim
Department of Medical Science
The Graduate School, Yonsei University

연세대학교
YONSEI UNIVERSITY

Physiological Roles of GRASP55 in Lipid Transport

Directed by Professor Min Goo Lee

The Doctoral Dissertation
submitted to the Department of Medical Science,
the Graduate School of Yonsei University
in partial fulfillment of the requirements for the degree of
Doctor of Philosophy

Jiyoon Kim

December 2017

연세대학교
YONSEI UNIVERSITY

This certifies that the Doctoral Dissertation of Jiyoon Kim is approved.

Thesis Supervisor: Min Goo Lee

Thesis Committee Member #1: Hoguen Kim

Thesis Committee Member #2: Jae Woo Kim

Thesis Committee Member #3: Sang Hak Lee

Thesis Committee Member #4: Heon Yung Gee

The Graduate School

Yonsei University

December 2017

ACKNOWLEDGEMENTS

2009년, 많은 고민 끝에 M.D.-Ph.D. 과정을 선택하기로 결심했을 때가 아직도 생생한데 벌써 9년이라는 시간이 지났다는 사실에 감회가 새롭습니다. 긴 학위 기간 동안 지금의 제가 있기까지 도와 주시고 격려해 주신 많은 분들께 깊은 감사의 말씀을 드립니다. 먼저 지난 5년간의 박사 학위 과정 동안, 탁월한 연구 능력으로 지도해 주시고 학자로서의 본을 보여주신 존경하는 이민구 교수님께 진심으로 감사의 말씀을 드립니다. 그리고 이번 학위 논문의 방향을 설정하는 데에 큰 도움을 주시고 뵐 때마다 격려해 주시는 김호근 교수님과 김재우 교수님, 논문 완성에 많은 도움을 주시고 졸업 후 진로에 대해서 진솔하게 상담해 주셨던 지헌영 교수님, 바쁘신 중에 학위 논문을 검토해 주신 이상학 교수님께 감사의 말씀을 드립니다. 또한 때마다 교실의 청사진을 제시해 주시는 김경환 교수님, 안영수 교수님, 김동구 교수님, 박경수 교수님, 복합학위 과정을 시작할 때부터 많은 동기 부여를 해 주시고 특히 박사후과정에 대해서 긴 시간 진솔하게 상담해 주셨던 김철훈 교수님, 저를 연구실 후배처럼 따뜻하게 대해주시는 김주영 교수님, 항상 반갑게 인사해주시는 김형범 교수님께도 지면을 빌어 감사드립니다.

연구를 진행하다 보면 실험이 뜻대로 되지 않고, 실험 결과를 이해하기 어려울 때가 많습니다. 동거동락한 연구실의 여러 선생님들이 아니었다면 그러한 어렵고 힘든 많은 순간들을 이겨내기가 참 힘들었을 것입니다. 먼저 저에게 많은 실험들을 가르쳐 주신 친누나 같은 신혜 누나, 든든한 버팀목이셨던 정남 누나, 그 뒤를 이어 랩 살림을 야무지게 잘 꾸리고 있는 소원이, 저를 아들처럼 생각해 주시는 김연정 선생님, 묵묵히 패치 방에 계시는 든든한 신동훈 선생님, 평생 같이 연구하기로 한 진세 형, 분위기 메이커 익현이 형, 다 잘 될 거라고 격려해 주셨던 한상이 형, 웨스턴 공장장

이라는 별명을 붙여 주셨던 형순이 형, 독일로 오라고 하시는 은석이 형, 연구 분야가 겹쳐서 많이 도와준 학이, 연구 분야가 안 겹쳐서 재미있게 얘기했던 준희 누나와 수민이, 의학도서관 최다 대여왕에 빛나는 강정민 선생님, 포근한 최성경 선생님, 마른 땅에 단비 같은 지훈이와 수경이, 신혜 누나를 잘 돕고 있는 가형이, 랩 단합의 큰 기둥이셨던 우영 누나, 일당백하던 운이, 이제는 같이 있기만 해도 좋은 형제 같은 준석이, 듣는 사람도 기분 좋게 웃는 정훈이, 잘 챙겨주는 친절한 요준이, 괴짜 과학자의 꿈을 이룰 것 같은 영익이, 귀여운 경지와 귀여운 세영이, 결혼 생활의 큰 지침을 주시는 김혜연 선생님, 모두 감사드립니다. 여러 선생님들의 도움 덕분에 지난 1년간 어려움 없이 랩 치프의 일을 할 수 있었습니다.

마지막으로, 변함 없는 사랑과 응원을 보내주시는 부모님, 장인 장모님, 말하지 않아도 마음을 잘 헤아려 주는 동생 지곤이, 가까이에서 가장 큰 기쁨과 위로와 평안을 주는 사랑하는 아내 희승님, 항상 기도해 주시는 방화동 교회 성도님들, 그리고 이 모든 일을 섭리하시고 인도하신 하나님께 감사드립니다. “자기의 유익을 구하지 말고, 남의 유익을 구하라 (고린도 전서 10:24)”라는 성경 구절을 지침으로 삼아, 더욱 의미 있는 연구들을 통해서 받은 은혜에 보답할 수 있도록 최선을 다하겠습니다.

TABLE OF CONTENTS

LIST OF FIGURES

LIST OF TABLES

ABSTRACT

Physiological Roles of GRASP55 in Lipid Transport

Jiyoon Kim

Department of Medical Science
The Graduate School, Yonsei University

(Directed by Professor Min Goo Lee)

The Golgi complex plays a key role in intracellular transport of proteins and lipids. This function is maintained under the fine regulation of various kinds of proteins. So far, most researches have been actively conducted on the Golgi-dependent protein trafficking. However, studies on the intracellular trafficking of lipids, especially, triglyceride (TG), are currently lacking. Here, we found that the Golgi reassembly stacking protein 55 (GRASP55), one of the Golgi-resident proteins, plays an essential role in the formation of chylomicron by regulating the targeting of the intestinal lipase, ATGL, into lipid droplets (LDs). These results indicate that the Golgi protein plays an important role not only in protein transport but also in lipid transport. Furthermore, by uncovering the new functions of GRASP55, this study provides a new insight into understanding the pathogenesis and therapeutics of various LD-associated diseases.

Key Words: GRASP55, Golgi complex, chylomicron, lipid droplet, ATGL

Physiological Roles of GRASP55 in Lipid Transport

Jiyoon Kim

Department of Medical Science
The Graduate School, Yonsei University

(Directed by Professor Min Goo Lee)

I. INTRODUCTION

Most proteins and lipids are transported from the endoplasmic reticulum (ER) to the Golgi complex via vesicular machineries[1-3], and then secreted into the plasma membrane, cytoplasm and cellular organelles[4]. Studies on intracellular trafficking of proteins and lipids have been tightly associated with understanding of vesicular proteins and their functions[5]. The understanding of the mechanism on intracellular trafficking pathways has been increasing[6]. The Golgi complex plays a central role in post-translational modifications of proteins and maturation of lipids[7,8]. Because of this importance, various Golgi-associated proteins including GRASP have been intensively studied [9-12].

The two vertebrate GRASPs, GRASP55 and GRASP65, were identified as major components required for post-mitotic remodeling of the Golgi cisternae[13-15]. In most eukaryotic cells, the Golgi complex is composed of several flat cisternae arranged in the later direction, forming a ribbon-like structure of stacks[10,16], and GRASPs are involved in Golgi stacking and ribbon-linking[15,17,18]. The Golgi complex is the cellular hub to accomplish a scrupulous transport of secretory cargo in the route from the ER

to the plasma membrane or other destinations[7,8]. Interestingly, it has been found that GRASPs appear to be involved in several other cellular processes including the protein sorting[19] and the unconventional protein secretion pathways[20-26]. These results suggest that GRASP proteins have diverse functions other than the function of maintaining the structure of the Golgi[20,27].

Previous studies on intracellular transport pathways have focused mainly on proteins. However, little is known about the intracellular transport of lipids, especially TG[28]. The molecular mechanism of how external triglycerides are packed into chylomicrons in the small intestine and enter the systemic circulation remains elusive. It has been reported that some of the absorbed lipids are stored in the form of lipid droplets (LDs) which function as lipid sources for the chylomicron during the post-prandial period[29]. It has been also found that a various proteins are specifically transported on the surface of LDs[30-38] and that LDs interact with other cellular compartments such as the ER[39-42], the ER-Golgi intermediate compartments (ERGIC)[43], the Golgi[44,45], mitochondria[46-48], peroxisome[49], endosome[50], plasma membrane[48], autophagosome[51] and ribosome[52,53] through intracellular motility, which suggests that LDs are distinct intracellular organelles. LDs have a unique structure with a hydrophobic core of neutral lipids surrounded by a monolayer phospholipid membrane[54]. A numerous interesting studies on how these structural properties regulate formation, growth, maintenance and extinction of LDs have been accumulated[55-57]. LDs are the key component in the regulation of intracellular lipid homeostasis, which contributes to the regulation of lipid balance throughout the tissue and organism[58]. Since the regulation of physiological function of LD is carried out by various kinds of proteins that coat the LD membrane, it is essential to understand the origin, intracellular trafficking and dissociation mechanism of LD-associated proteins to define the characteristics of LDs. In addition, recent studies on the relationship between LDs and various metabolic diseases have raised the importance of the pathophysiological role of LD[57,59-61]. However, despite the importance of LDs, no consensus has yet been reached on the molecular mechanism of LD formation and regulation.

In the current study, we explore the new function of GRASP55 in the intestinal trafficking of lipid by demonstrating GRASP55 plays a critical role in lipid homeostasis by regulating cellular localization of ATGL and its targeting to LD. These results provide new insights into the unconventional role of the Golgi protein in formation of chylomicron to regulate biogenesis of LDs. Furthermore, identification of GRASP55 as a new regulator for lipid droplets will make a contribution to therapeutic strategies for LD-associated diseases.

II. MATERIALS AND METHODS

1. Animals and care

Grasp55$^{-/-}$ mice were purchased from the Jackson Laboratory. All experiments were performed using male Grasp55$^{-/-}$ mice and their corresponding control littermates. Mice had free access to food and water under a 12-h light/12-h dark cycle in a temperature controlled environment. The high-fat diet contained 60% kcal% fat (D12492, Research Diets, New Brunswick, NJ, USA). All animal experiments were approved by the Institutional Animal Care and Use Committees (IACUC) in Yonsei University College of Medicine (Animal protocol #2016-0106), Republic of Korea.

2. Cell line and Cell culture

Caco-2 cells were maintained in Dulbecco's modified Eagle's medium (DMEM high glucose) containing 20% fetal bovine serum (FBS), penicillin (50 IU/mL)/ streptomycin (50 μg/mL), 2mM L-glutamine and non-essential amino acid (all from Invitrogen, Waltham, MA, USA) in 5% CO_2 incubator at 37℃. To generate Grasp55 knock-down stable cell line, Caco-2 cell was transducted with lentiviral particles produced from HEK293T cell which were transfected with psPAX2 packing plasmid, pMD2.G envelope plasmid and pLKO.1 short-hairpin RNA (shRNA) plasmid (control shRNA : #SHC001, Gorasp2-specific shRNA : #TRCN0000127674 ; Yonsei Genome Center, Seoul, Korea) and selected using puromycin. To induce LDs, Caco-2 cells were oil-loaded with DMEM containing oleic acid:BSA complex (final concentration 4:1 mM) for 16hr before harvest.

3. Antibodies

Antibodies were from the following sources: anti-ApoA1 (ab33470), anti-ApoA4 (ab59036), anti-ApoE (ab183597), anti-ApoB (ab31992), anti-CIDEB (ab9403), anti-Giantin (ab93281), anti-GM130 (ab52649), anti-Calreticulin (ab92516), anti-Grasp55 (ab74579), anti-LMAN1 (ab125006), anti-Arf1 (ab183576), anti-ARFRP1 (ab108199,

Abcam, Cambridge, MA, USA), anti-Albumin (#4929), anti-Syntaxin 6 (#2869), anti-HSL (#4107), anti-phosphoHSL (Ser563, #4139), anti-ATGL (#2138, Cell Signaling Technology, Danvers, MA, USA), anti-ADRP (LS-C3561), anti-TIP47 (LS-B671), anti-MTTP (LS-C144891, LSBio, Seattle, WA, USA), anti-GBF1 (NBP1-06526, Novus Biologicals, Littleton, CO, USA), anti-aldolase A (sc-12059), anti-actin (sc-1616, Santa Cruz Biotechnology, Santa Cruz, CA, USA) and anti-TGN38 (AHP1597, BIO-RAD, Hercules, CA, USA)

4. Immunoblotting

Immunoblotting was performed as described previously[62]. Cells were homogenized in lysis buffer containing 50 mM Tris pH 7.4, 1% (v/v) NP40, 150 mM NaCl, 1 mM EDTA supplemented with protease inhibitor mixture (Roche, Applied Science, Mannheim, Germany). For tissues, lysis buffer contained additional 100 mM benzamidine and 0.3% soybean trypsin I. Protein samples were separated by SDS-polyacrylamide gel electrophoresis. The separated proteins were transferred to a nitrocellulose membrane and blotted with appropriate primary and secondary antibodies. Protein bands were detected by enhanced chemiluminescence (ECL) and the densities of the bands were measured using imaging software (ImageJ, National Institutes of Health, USA, http://imagej.nih.gov/ij).

5. Immunohistochemistry, Immunocytochemistry and Confocal microscope image acquisition

Immunohistochemistry was performed as previously reported[24]. Jejunum was isolated and fixed in 10% neutral-buffered formalin (HT501128, Sigma Aldrich, St. Louis, MO, USA). Paraffin sections of the jejunum were cut and antigen retrieval was performed by heat treatment. Unspecific binding sites were blocked with 5% donkey serum, 1% BSA and 0.1% gelatin in PBS for 30min. The indicated primary antibodies were applied overnight at 4℃. Tissues were treated with fluorophore-dye conjugated secondary antibodies. Fluorescence images were captured using a laser scanning confocal microscope with a 40x 1.4 numerical aperture (NA) water objective lens

(LSM 780, Carl Zeiss, Berlin, Germany). To stain the lipid components, paraffin slide of the jejunum was stained with Oil Red O and Mayer's hematoxylin. Microscopic images were taken using a Nikon Eclipse E600 equipped with a Nikon Digital Sight DS-U1 unit (Spach Optics Inc., New York, NY, USA).

Immunocytochemistry was performed as previously reported[62]. Caco-2 cells were cultured on 18 mm round coverslips and fixed with 10% formalin for 10 min at room temperature. The fixed cells were washed three times with PBS and then were permeabilized with 0.1% Triton X-100 for 15 min at room temperature. Cells were incubated with blocking solution containing 5% donkey serum, 1% BSA and 0.1% gelatin in PBS for 30 min at room temperature. After the blocking step, cells were stained by incubating with appropriate primary antibodies overnight at 4℃. Cells were treated with fluorophore-dye conjugated secondary antibodies. LD staining with BODIPY 493/503 was performed as previously reported[63]. Fluorescence images were captured using a laser scanning confocal microscope with a 63x 1.4 numerical aperture (NA) oil objective lens (LSM 780).

6. Transmission electron microscopy

Jejunum and liver were fixed with 2.5% glutaraldehyde and 2% paraformaldehyde. Samples were rinsed in 0.1 M phosphate buffer and post-fixed with 1% osmium tetroxide, dehydrated in ascending concentrations of methanol and propylenoxide and embedded into Epoxy resin. Blocks were trimmed, sectioned and viewed on the FEI EM 208 transmission electron microscope at ×13 000 magnification. Negatives were scanned at 800 dpi.

7. Oil gavage and Oral fat tolerance test (OFTT)

Mice were fasted for 16hr and received 10 μl/body weight (g) olive oil by oral gavage. To perform OFTT, blood samples (30 μl) were collected via the tail vein prior to (basal, time 0), and 1, 2, 3 and 4hr after the oral oil application for the determination of plasma triglyceride using colorimetric assay kit (#10010303, Cayman Chemical Company, Ann Arbor, MI, USA) according to the manufacturer's

instruction.

8. Lipid and amino acid uptake assay

For differentiation, Caco-2 cells were maintained for 3 weeks on the transwell system with a medium change every 2 days and verified by measuring transepithelial electrical resistance. Differentiated Caco-2 cell was incubated with ^{14}C-labeled oleic acid (Moravek, California, CA, USA) in the apical part. After 16hr, the radioactivity was quantified in the basolateral medium and normalized to background radioactivity.

The amino acids uptake was measured as previously reported[64]. Grasp55$^{+/+}$ and Grasp55$^{-/-}$ mice were fasted for 16hr and received by gavage 10 μl/body weight (g) PBS solution containing amino acid mixture at a final concentration 100-fold higher than 1.5 μCi/ml ^{14}C-radiolabeled amino acid (Moravek, California, CA, USA). After 1hr, animals were sacrificed by cervical dislocation. The blood was collected by cardiac puncture and the radioactivity was determined.

9. Plasma parameter assay

Grasp55$^{+/+}$ and Grasp55$^{-/-}$ mice were fasted for 16hr and blood was collected by cardiac puncture. The several plasma parameters including triglyceride and total cholesterol were measured by using Fuji Dri-chem Nx500 (FUJIFLIM Co., Tokyo, Japan), according to the manufacturer's instruction.

10. Subcellular fractionation assay

Subcellular fractionation on OptiPrep^{TM} Density Gradient Medium (D1556, Sigma Aldrich, St. Louis, MO, USA) was performed as previously reported[62] with minor modifications according to the OptiPrep^{TM} users' manual. Mouse jejunum tissue was washed wish PBS, chopped into tiny pieces in cell suspension medium containing 0.85% (w/v) NaCl and 10mM tricine-NaOH (pH 7.4), and homogenized by repeated passage through a 30G syringe needle. The postnuclear supernatant was collected after centrifugation of the homogenates at 1500 × g for 10min and fractions were loaded on top of the density gradient solution containing 2.5–30% (w/v) OptiPrep^{TM}

in cell suspension medium. Subcellular organelles were separated by centrifugation using an Optima TLX ultracentrifuge (Beckman Coulter, Brea, CA, USA) with a SW41 swinging bucket rotor at 200,000 × g for 2.5 hr. Nine fractions were collected from the top to the bottom, and a 40 μl aliquot of each fraction was used for immunoblotting.

11. Fluorescence recovery after photobleaching (FRAP) assay

Isolation of mouse embryo fibroblasts (MEFs) was performed as previously reported[65]. Grasp55$^{+/+}$ and Grasp55$^{-/-}$ mice MEFs were transfected with the mammalian expression plasmid enhanced yellow fluorescent protein (EYFP) using TransIT-X2 Dynamic Delivery System (Mirus Bio LLC, Madison, WI, USA). After the part of the Golgi was bleached using a single laser pulse, images were captured every 5sec using a laser scanning confocal microscope with a 63x 1.4 numerical aperture (NA) oil objective lens (LSM 780) and normalized to total cellular fluorescence.

12. Statistical analysis

All experiments were performed at least three times independently for each condition and presented as the mean ±standard deviation (SD). Statistical significance was determined using Student's *t*-test. $p < 0.05$ was considered statistically significant. Calculations were performed using GraphPad Prism5 software (GraphPad Software, La Jolla, CA, USA).

III. RESULTS

1. The deficiency of Grasp55 causes growth retardation and decreases body fat *in vivo*

Mice lacking Grasp55 (Grasp55$^{-/-}$) were born with differences in size compared to their wild-type siblings. The growth retardation of Grasp55$^{-/-}$ mice lasted from the birth to the 30-week-old (Figure 1A). In particular, after about 12 weeks of age corresponding to the young adult period, the body weight of Grasp55$^{-/-}$ male mice did not increase further at about 20g (Figure 1B). However, survival rate of Grasp55$^{-/-}$ was normal (Figure 1C). The weights of major organs including liver, kidney, and intestine were significantly reduced in Grasp55$^{-/-}$ mice. The relative ratio of most organs weight to body weight showed no significant difference between control (Grasp55$^{+/+}$) and Grasp55$^{-/-}$ mice. However, the relative ratio of white adipose tissue (WAT) and brown adipose tissue (BAT) was still significantly reduced (Table 1). Therefore, we focused on adipose tissues. Epididymal white adipose tissue, a representative part of visceral fat[66], was scarcely found in Grasp55$^{-/-}$ mice, and the size of adipocytes was significantly reduced in H&E staining (Figure 2A). BAT of the Grasp55$^{-/-}$ mice was also decreased in the size of both tissue and adipocytes (Figure 2B). The levels of serum lipids such as triglycerides and total cholesterol were also lower than those of control mice (Table 2). Interestingly, after high-fat diet for 11 weeks, epididymal white adipose tissue of Grasp55$^{-/-}$ mice was still significantly reduced compared to control mice (Figure 2C-E), suggesting that Grasp55$^{-/-}$ mice were resistant to weight gain induced by high-fat diet. In the H&E staining of liver tissue, Grasp55$^{-/-}$ showed no significant difference from control mice (Figure 2F). However, in ultrastructural analysis using electron microscopy, hepatic lipid droplets were decreased in Grasp55$^{-/-}$ (Figure 2F). Moreover, when the amount of triglyceride present in a certain amount of liver tissue was measured, the amount of triglyceride in Grasp55$^{-/-}$ liver tissue was significantly lower than that of control mice (Figure 2G).

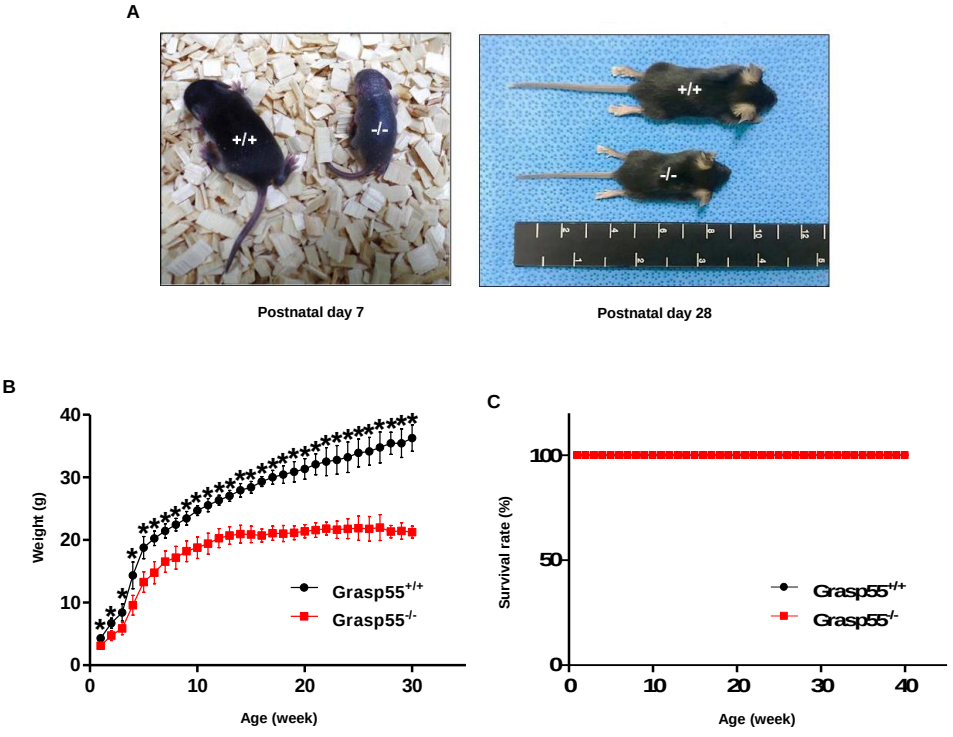

Figure 1. Growth retardation and survival rate of Grasp55$^{-/-}$ mice. (A) Photographs of 7- and 28-day-old Grasp55$^{+/+}$ and Grasp55$^{-/-}$ mice. **(B)** Body weights of Grasp55$^{+/+}$ and Grasp55$^{-/-}$ mice at the age of 1-30 weeks (n=15). **(C)** Survival curves of Grasp55$^{+/+}$ and Grasp55$^{-/-}$ mice that were fed with a standard diet over a time period of 40 weeks (n=15) (*p <0.001).

Table 1. The relative proportions of major organs of Grasp55$^{+/+}$ and Grasp55$^{-/-}$ mice (male, 4-week-old, n=6, g/[body weight(g)], %)

	GRASP55$^{+/+}$	GRASP55$^{-/-}$	p-value
White Adipose Tissue	0.48 ± 0.02	0.09 ± 0.03	0.0003
Brown Adipose Tissue	0.28 ± 0.01	0.18 ± 0.02	0.0113
Liver	5.00 ± 0.44	4.25 ± 0.54	0.3415
Kidney	1.56 ± 0.01	1.40 ± 0.14	0.3949
Intestine	7.00 ± 0.15	7.17 ± 0.27	0.6392
Colon	1.67 ± 0.06	1.51 ± 0.07	0.1449
Lung	0.90 ± 0.02	0.75 ± 0.11	0.2625
Heart	0.80 ± 0.06	0.66 ± 0.05	0.1491
Skeletal muscle	1.11 ± 0.08	1.13 ± 0.11	0.8901

Table 2. Plasma parameters of Grasp55$^{+/+}$ and Grasp55$^{-/-}$ mice (male, 12-week-old, n=6)

	GRASP55$^{+/+}$	GRASP55$^{-/-}$	p-value
Triglycerides (mg/dL)	79.00 ± 2.85	63.28 ± 3.48	0.0023
Total Cholesterol (mM)	2.63 ± 0.10	1.69 ± 0.09	<0.0001
Glucose (mg/dL)	115.00 ± 5.48	115.80 ± 2.62	0.8838
ALT (U/L)	33.33 ± 6.03	82.00 ± 14.24	0.0028
AST (U/L)	106.67 ± 17.01	151.00 ± 8.54	0.0157
Albumin (g/dL)	2.65 ± 0.40	2.88 ± 0.28	0.3930
Total bilirubin (mg/dL)	0.65 ± 0.30	1.03 ± 0.06	0.1654
Total protein (g/dL)	5.73 ± 0.53	5.45 ± 0.07	0.5294

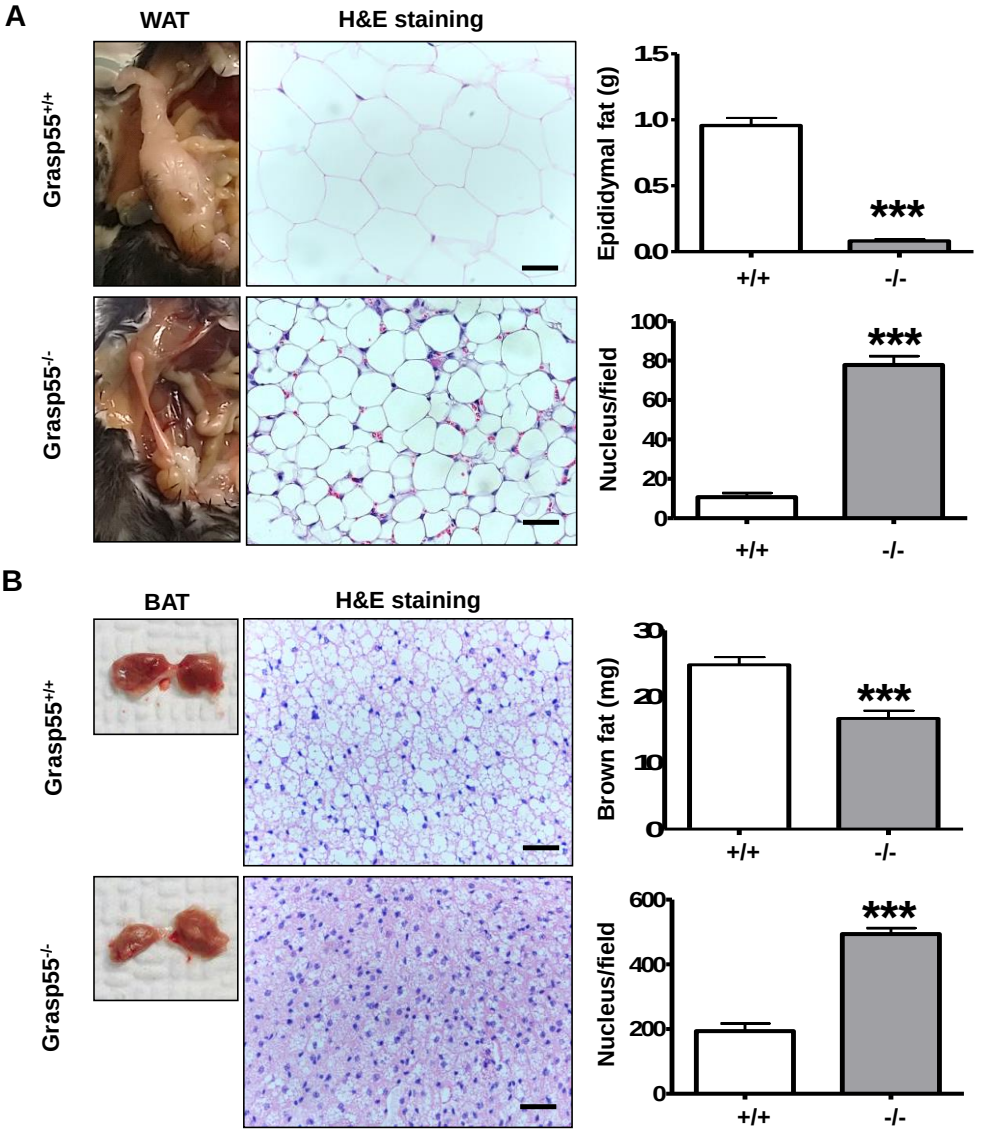

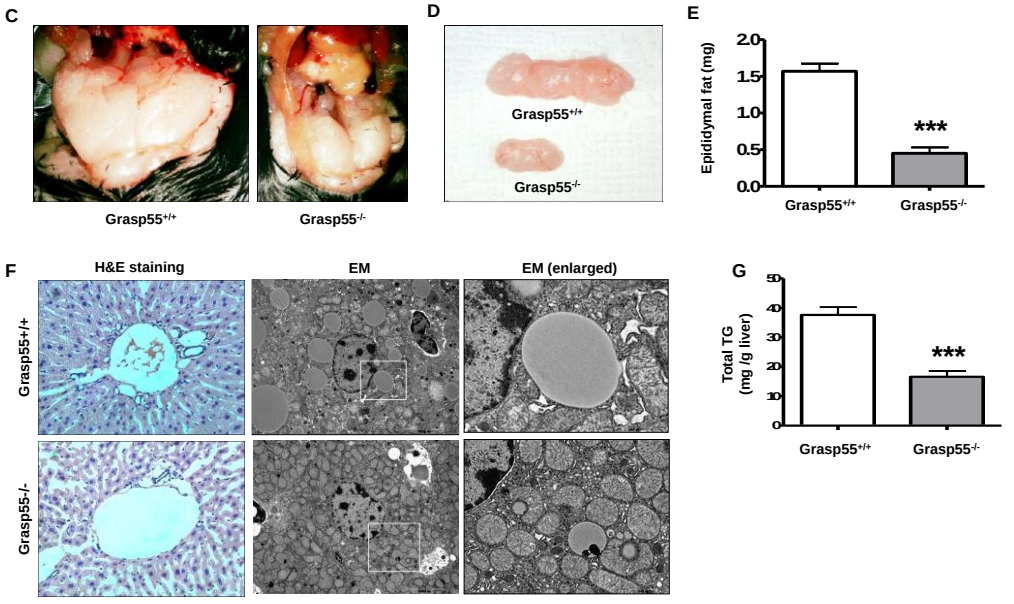

Figure 2. Lack of lipids in adipose and liver tissues of Grasp55$^{-/-}$ mice. (A) Ventral view (left panel) and H&E staining (middle panel) of epididymal fat of Grasp55$^{+/+}$ and Grasp55$^{-/-}$ littermates at the age of 12 weeks. Reduced fat weight (n=6; right, upper) and size of adipocytes (n=10; right, lower) were quantified. **(B)** Brown adipose tissues of Grasp55$^{+/+}$ and Grasp55$^{-/-}$ littermates at the age of 12 weeks (n=6). Other experimental conditions were the same as in panel (A). **(C)** Ventral view of epididymal fat of Grasp55$^{+/+}$ and Grasp55$^{-/-}$ mice at the age of 20 weeks after high-fat diet for 11 weeks. **(D)** Photograph of one side epididymal fat of Grasp55$^{+/+}$ and Grasp55$^{-/-}$ mice. **(E)** The weights of one side epididymal fats in Grasp55$^{+/+}$ and Grasp55$^{-/-}$ mice were quantified (n=6). **(F)** H&E staining and ultrastructural analysis of liver of Grasp55$^{+/+}$ and Grasp55$^{-/-}$ littermates at the age of 16 weeks after 16hr fasting. **(G)** The concentrations of triacylglycerol (TG) in liver of Grasp55$^{+/+}$ and Grasp55$^{-/-}$ were measured. Scale bars: 50 μm. Data shown are mean±SEM. ***$p<0.001$.

2. Lack of Grasp55 reduces intestinal fat absorption

To investigate the cause of the decrease of adipose tissue and plasma lipid concentration in Grasp55$^{-/-}$ mice, we examined intestinal fat absorption. After 16hr fasting, morphology of intestinal epithelium between control and Grasp55$^{-/-}$ mice was compared. There were no differences between control and Grasp55$^{-/-}$ mice, and there were no significant differences in by H&E staining and lipid staining with Oil Red O (Figure 3A). However, after the oral olive oil application, numerous vesicles were found in H&E staining of Grasp55$^{-/-}$ mice intestine (Figure 3B, left panel). In addition, these vesicles were also found to contain lipid components by staining with Oil Red O (Figure 3B, right panel).

Next, oral fat tolerance tests with 5-week-old mice indicated an impaired lipid absorption in Grasp55$^{-/-}$ mice, showing a failure to respond to a bolus of olive oil by an increase in plasma triacylglycerol in contrast to controls (Figure 4A). Additionally, to test the impact of GRASP55 on fat absorption *in vitro*, we established Caco-2 stable cell line of which Grasp55 expression was stably suppressed (shGrasp55; Figure 4B, lane 2). Both differentiated normal and shGrasp55 Caco-2 cells were incubated with ^{14}C-labeled oleic acid and radioactive oleic acid was measured in each basolateral chamber. The release of fatty acid to the basolateral chamber was significantly reduced in shGrasp55 Caco-2 cells (Figure 4C), suggesting that the basolateral export of lipid is defective upon the disruption of Grasp55. However, there was no significant difference in the absorption of amino acids between Grasp55$^{+/+}$ and Grasp55$^{-/-}$ (Figure 4D-F).

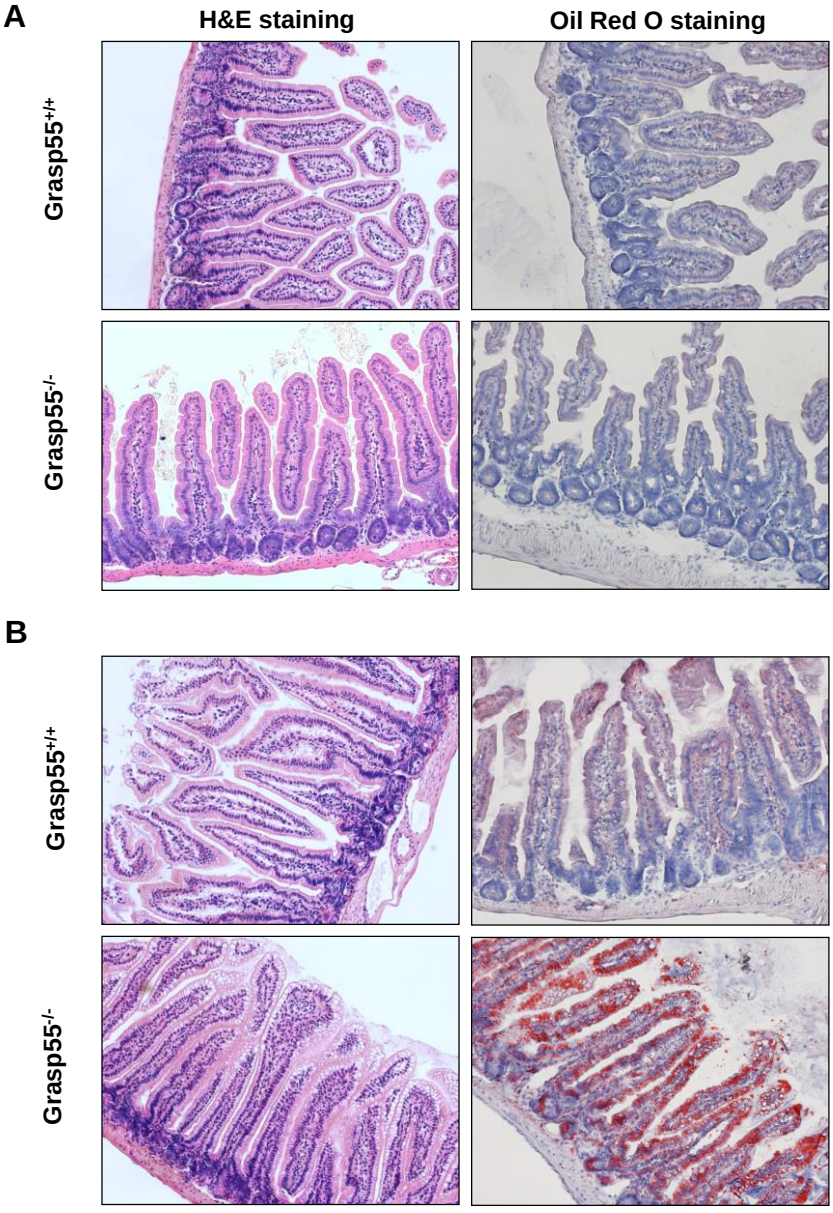

Figure 3. Intestinal lipid accumulation in Grasp55$^{-/-}$ mice. H&E staining (left panel) and Oil Red O staining (right panel) of jejunum in mice fasted for 16hr **(A)** or 4hr after oral gavage of olive oil **(B)**. Scale bars: 50 μm.

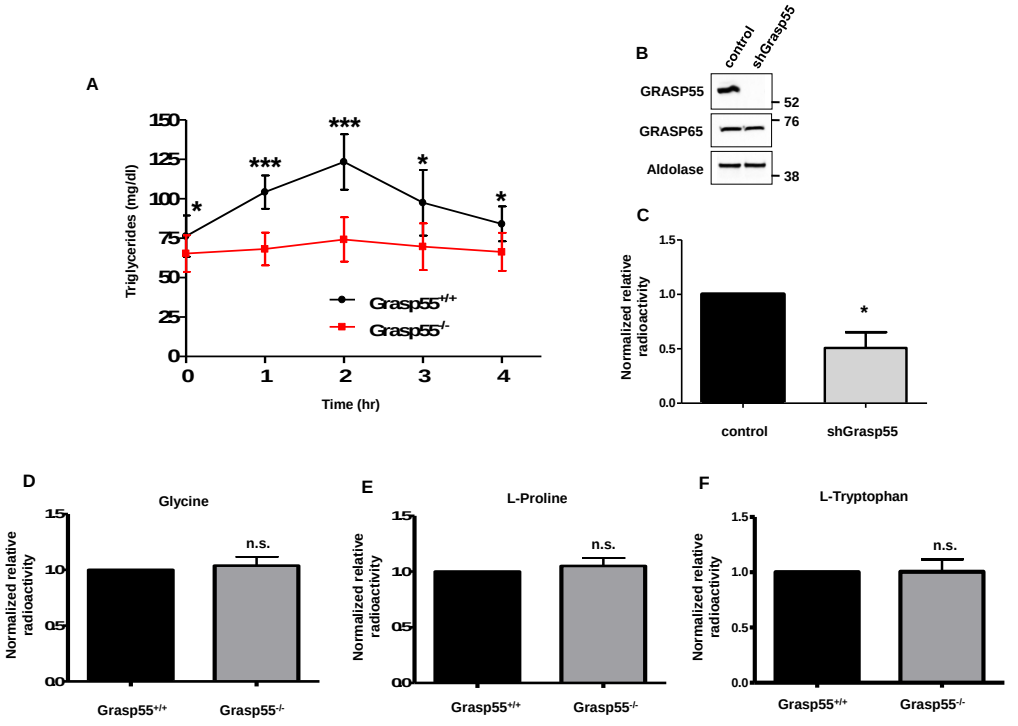

Figure 4. Triacylglycerol and amino acids absorption in depletion of Grasp55. (A) Triacylglycerol concentrations during fat tolerance tests with 8-week-old Grasp55$^{+/+}$ and Grasp55$^{-/-}$ mice (n=6). **(B)** Caco-2 stable cells of which Grasp55 expression was significantly suppressed were subjected to western blot analysis. **(C)** Impaired lipid release of Caco-2 cells after the down-regulation of Grasp55 expression. Caco-2 cells were differentiated as described in Materials and Methods. Cells were incubated with ^{14}C-labeled oleic acid for 24hr, and radioactivity was determined in the basolateral medium reflecting the release (n=6). **(D-F)** The absorption of amino acids including glycine **(D)**, L-proline **(E)**, L-tryptophan **(F)** in Grasp55$^{-/-}$ mice showed no difference with that of Grasp55$^{+/+}$ mice. Grasp55$^{+/+}$ and Grasp55$^{-/-}$ littermates were received by oral gavage with radiolabeled amino acids. Radioactivity in the plasma was determined 1hr after gavage (n=4). Data shown are mean±SEM. n.s. : non-significant, *p<0.05, ***p<0.001.

3. Grasp55$^{-/-}$ mice have impairment of chylomicron secretion

Next, the blood of Grasp55$^{-/-}$ mice was analyzed to elucidate what kind of component among various lipids was defective. Fractionation of lipids into chylomicrons, IDL, LDL and HDL by FPLC revealed a predominant decrease in triglycerides concentrations in the chylomicron/VLDL fraction of Grasp55$^{-/-}$ mice after oil bolus (Figure 5A). Ultrastructural analysis of intestinal epithelial cells demonstrated that deficiency of Grasp55 leads to an enlarged size but a lower number of chylomicrons (arrows in Figure 5B) in the Grasp55$^{-/-}$ epithelial cell (quantification shown in Figure 5C). After fatty acids are converted to triacylglycerol, they are coated with several proteins including apolipoprotein B100 (ApoB100), apolipoprotein B48 (ApoB48), apolipoprotein A1 (ApoA1), apolipoprotein A4 (ApoA4) and apolipoprotein E (ApoE), forming either chylomicrons or very-low-density lipoproteins (VLDLs)[67,68]. We determined their levels in the plasma of control and Grasp55$^{-/-}$ mice after fasting or 4hr after an olive oil bolus. Fasting plasma ApoB100 and B48 levels of Grasp55$^{-/-}$ mice were significantly reduced compared with control mice (Figure 5D, lane 1 and 2). In addition, the plasma ApoB100, but not B48, level in control mice increased after the lipid application (Figure 5D, lane 1 and 3). Grasp55$^{-/-}$ mice showed the increase of both plasma ApoB100 and ApoB48 expression in response to olive oil bolus (Figure 5D, lane 2 and 4). Plasma concentrations of ApoA1, ApoA4 and ApoE were not affected by oil bolus and Grasp55 deficiency (Figure 5D) (quantification shown in Figure 5E).

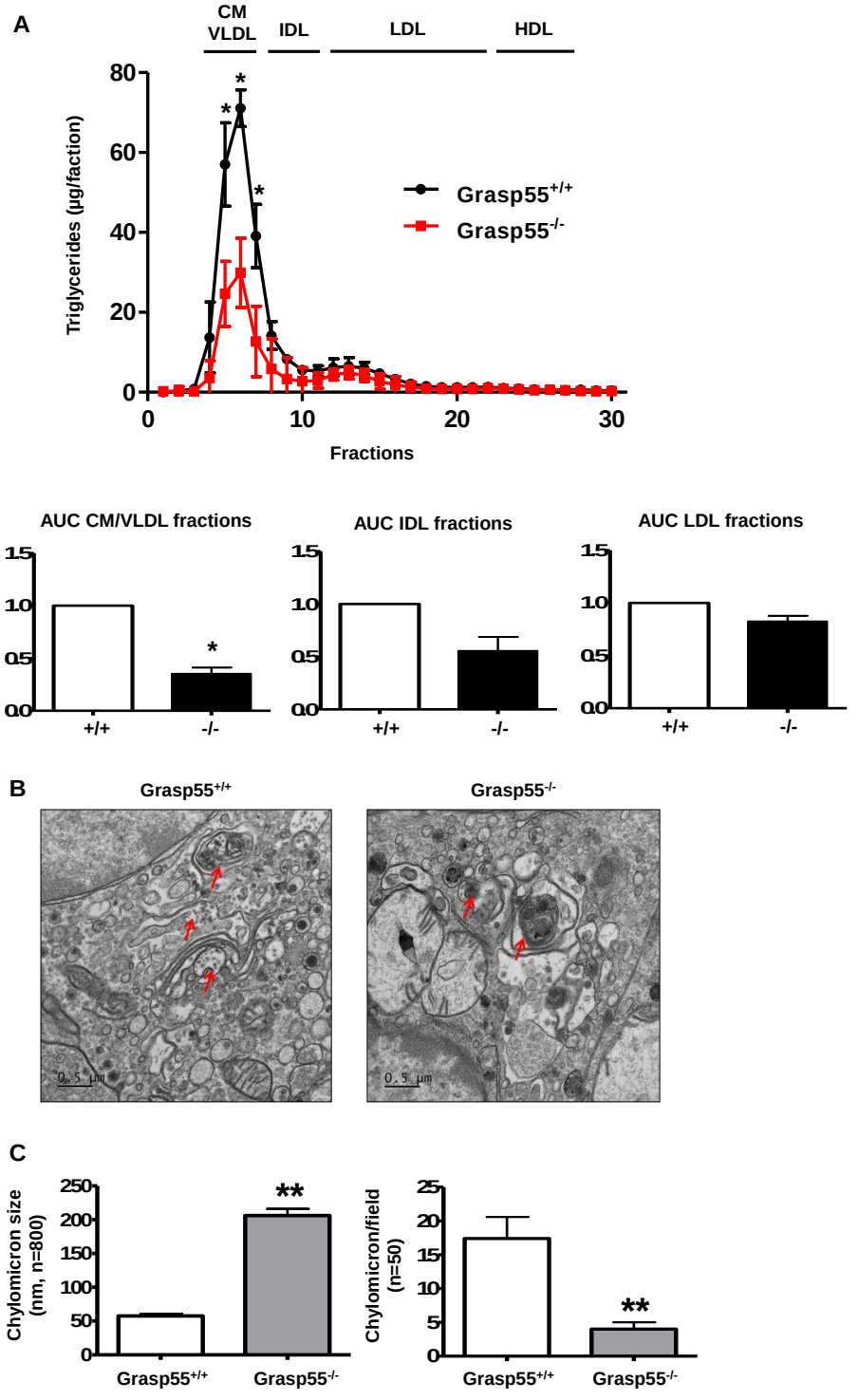

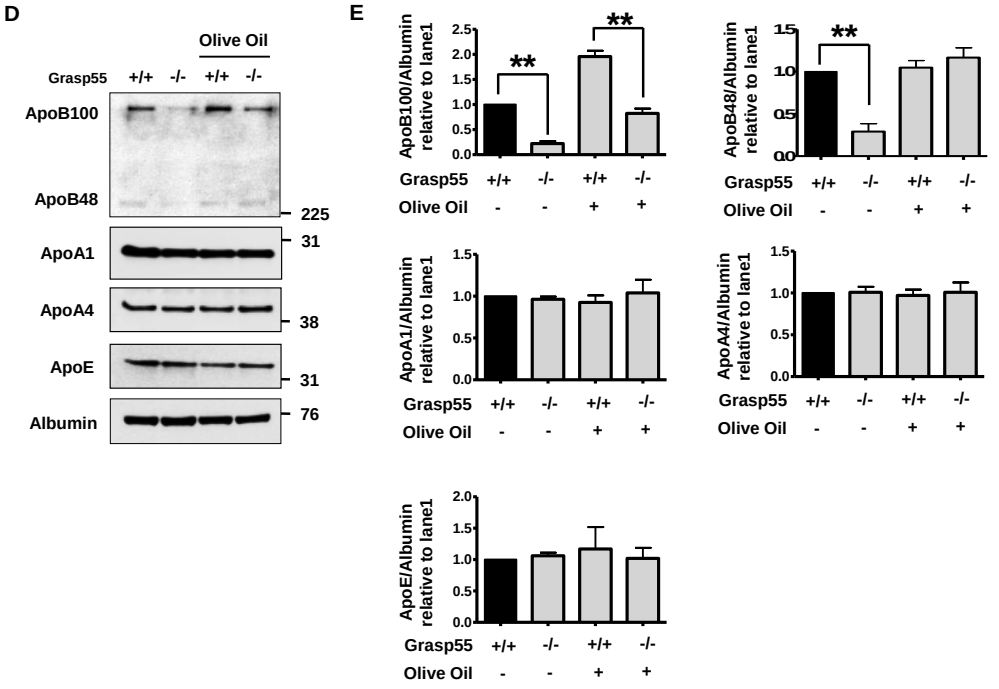

Figure 5. Reduced fat absorption and chylomicron secretion in Grasp55$^{-/-}$ mice. **(A)** FPLC profiles of plasma samples of Grasp55$^{+/+}$ and Grasp55$^{-/-}$ mice (n=3, 3-4 mice plasma pooling/n) that received an oil bolus. Triacylglycerol (μg) was detected in the different fractions, chylomicron/VLDL (fractions 4–7), IDL (fractions 8-11), LDL (fractions 12–22) and HDL (fractions 23–30) (CM: chylomicrons, AUC: area under curve). **(B)** Ultrastructural analysis of intestinal epithelial cells of Grasp55$^{+/+}$ and Grasp55$^{-/-}$ mice. Pictures show representative Golgi structures of epithelial cells. The arrows indicate chylomicrons that were visible in normal size in control cells but were enlarged in Grasp55$^{-/-}$ cells. **(C)** Quantification of the diameter (left graph) and number (right graph) of chylomicrons seen in the observed area in epithelial cells of Grasp55$^{+/+}$ and Grasp55$^{-/-}$ mice. **(D)** Plasma of 16hr fasted Grasp55$^{+/+}$ and Grasp55$^{-/-}$ mice (lane 1 and 2) or of mice 2hr after receiving an oil bolus (lane 3 and 4) was analyzed by western blotting with the indicated antibodies. The level of albumin was monitored as a loading control. The results of multiple experiments (n=6) are summarized in **(E)**. Data shown are mean±SEM (*p<0.01, **p<0.001).

4. Cytoplasmic lipid droplets are accumulated in the Grasp55$^{-/-}$ intestinal epithelium

To determine the cause of the chylomicron secretion defect, we investigated cellular localization of apolipoproteins using immunofluorescence. After fasting, there were no differences in intestinal localization of ApoB, ApoA1 and ApoA4 between control and Grasp55$^{-/-}$ mice (Figure 6A-C, 'fasting'). However, 4hr after an olive oil bolus, the expression of ApoB and ApoA4 was enhanced, and ApoA1 spread to the basolateral area (Figure 6A-C, 'oil application'). In particular, large structures like vesicles were observed in the intestinal epithelium of Grasp55$^{-/-}$ mice. Interestingly, when staining with TiP47, one of the lipid droplet markers, the vesicle boundaries were clearly stained (Figure 6D, right panel). These results suggest that the supersized vesicles in the epithelium of Grasp55$^{-/-}$ mice received an olive oil are LDs. On the electron microscope, a small number of small LDs were observed after the olive oil bolus in control mice, while a relatively small number but huge LDs were observed in the Grasp55$^{-/-}$ mice (Figure 6E). Next, in order to investigate the cause of these huge LDs, we compared intestinal protein expression by western blotting. Lipid-sensing apolipoproteins such as ApoA4 and ApoE were normally induced by an oil bolus both in control and Grasp55$^{-/-}$ mice (Figure 6F, lane 3 and 4). However, quantitative expression changes of apolipoproteins including ApoB100, ApoB48, ApoA1, ApoA4 and ApoE were not found by Grasp55 deficiency (Figure 6F) (quantification shown in Figure 6G).

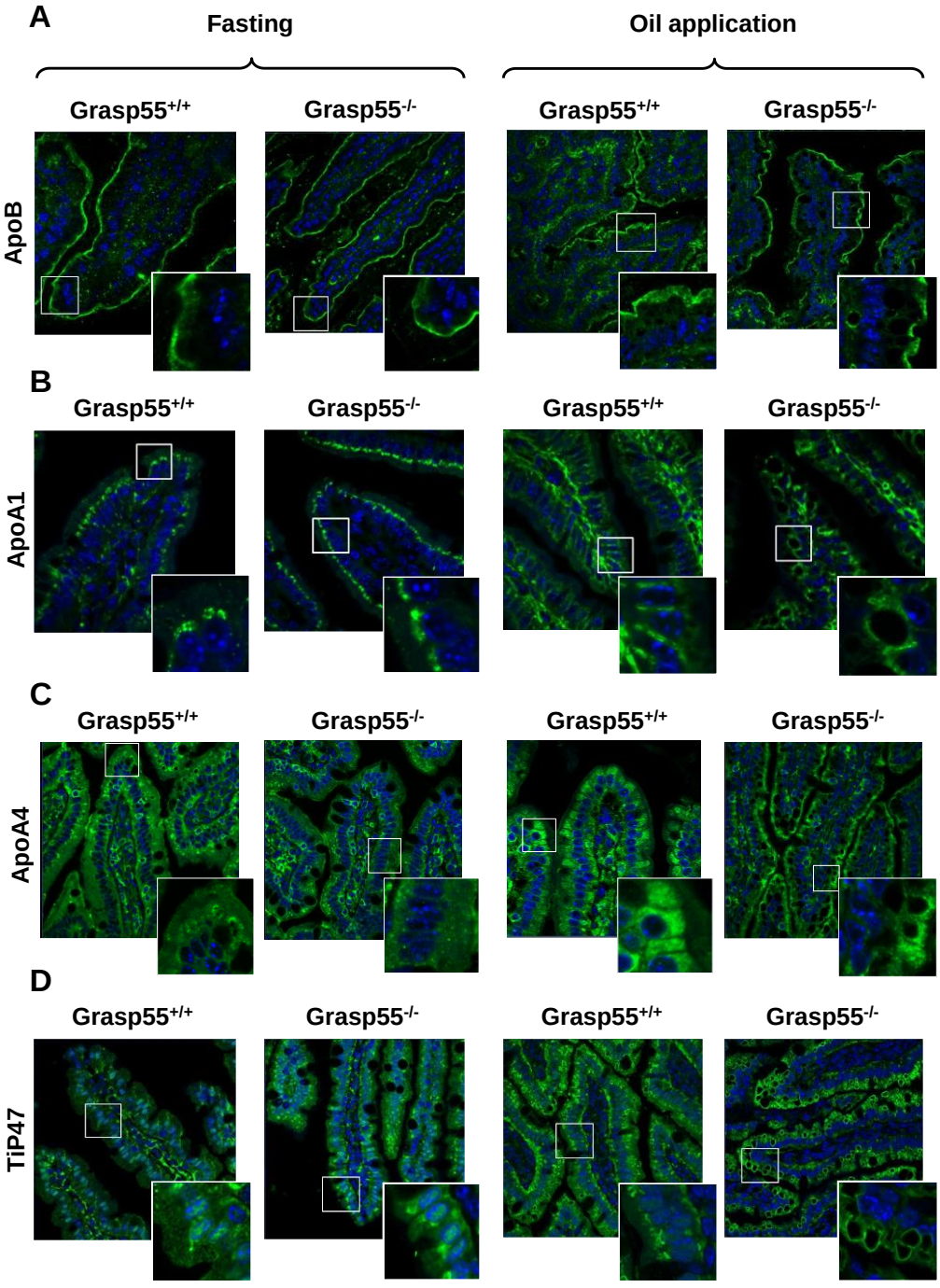

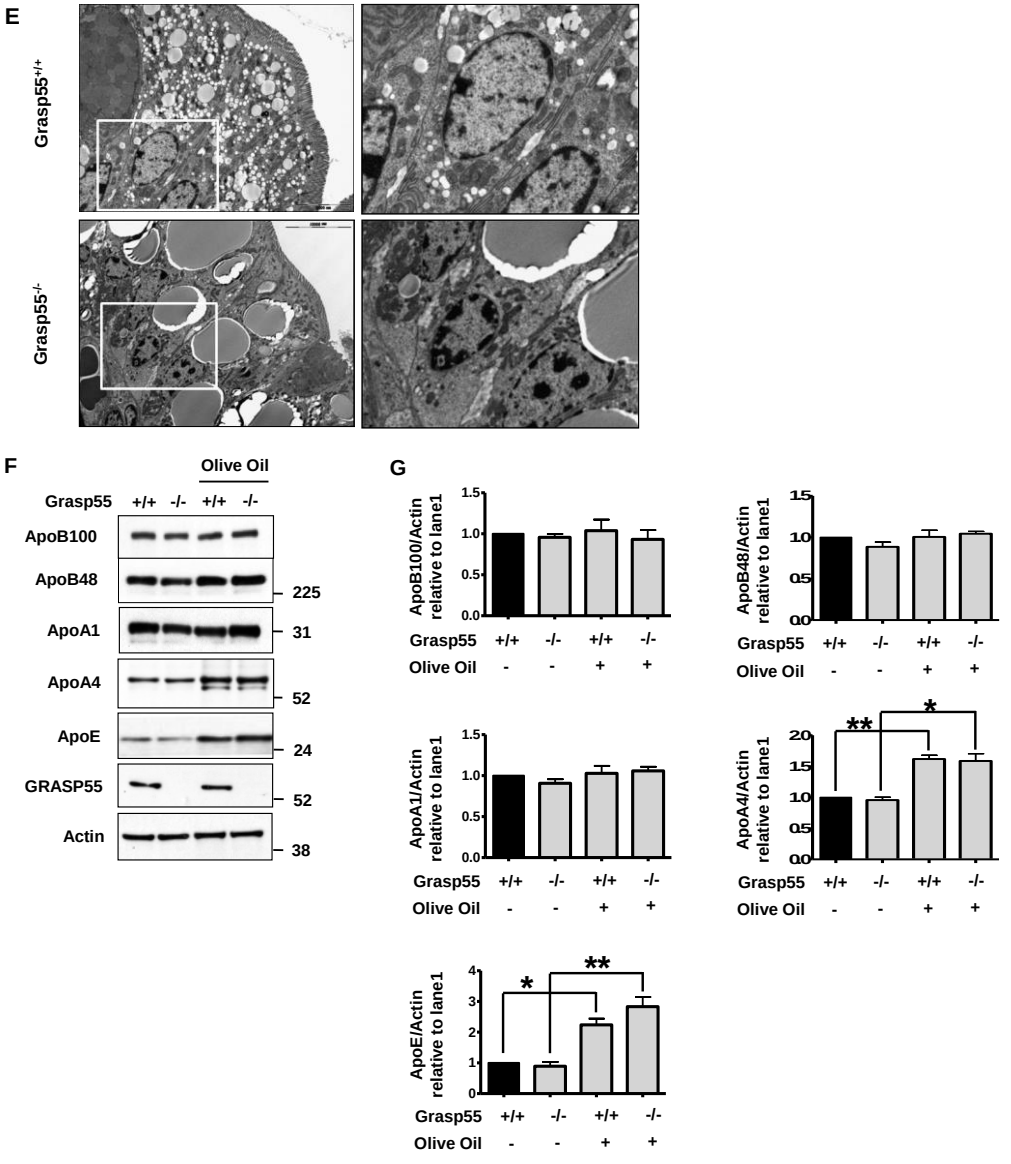

Figure 6. Expression analysis of chylomicron or lipid droplet-associated proteins in intestinal epithelium from Grasp55$^{+/+}$ and Grasp55$^{-/-}$ littermates. (A-D) Immunohistochemical detection of indicated apolipoproteins and TiP47 in the intestinal section of Grasp55$^{+/+}$ and Grasp55$^{-/-}$ mice fasted (left panels, 'Fasting') or after the olive oil bolus (right panels, 'Oil application'). Nuclei were counterstained with 4, 6-diamidino-2-phenylindole (DAPI). Images acquisition for all was performed

with the same settings. **(E)** Ultrastructural analysis of intestinal epithelial cells of Grasp55$^{+/+}$ and Grasp55$^{-/-}$ mice. **(F)** Intestinal apolipoprotein expression of 16hr fasted Grasp55$^{+/+}$ and Grasp55$^{-/-}$ mice (lane 1 and 2) or of mice 4hr after receiving an oil bolus (lane 3 and 4) was analyzed by western blotting with the indicated antibodies. The level of actin was monitored as a loading control. The results of multiple experiments are summarized in **(G)**. Data shown are mean±SEM (n=6, *$p<0.05$, **$p<0.01$).

5. GRASP55 regulates the cellular localization, protein expression and stability of ATGL

Since we could not detect any defect of cellular localization and protein expression of apolipoproteins, we screened other proteins associated with chylomicrons and LDs. First, we investigated changes in subcellular localization of apolipoproteins (ApoB, ApoA1, ApoA4), other proteins involved in lipidation of chylomicron such as ARFRP1[69], CideB[70], MTP[71], and LD-associated lipases such as HSL[72] and ATGL[43,73] by fractionation the ER and the Golgi resident proteins with OptiPrep™ density gradient (Figure 7A). Surprisingly, the localization of ATGL showed difference between control and Grasp55$^{-/-}$ mice. However, there was no change in the localization of GBF1 and ARF1, known ATGL regulators[33,43,74].

To confirm these results of the subcellular fractionation, we examined the cellular localization of intestinal ATGL by immunohistochemistry. The deficiency of Grasp55 diminished co-localization between ATGL and the Golgi marker, and these results were especially more evident after olive oil bolus (Figure 7C) than after normal diet (Figure 7B).

Next, we examined the intestinal expression of ATGL by western blotting. In control mice, protein expression of ATGL was increased by olive oil bolus (Figure 8A, lane 1 and 3). However, ATGL expression of Grasp55$^{-/-}$ mice was significantly decreased even with normal diet compared to control mice and failed to increase in response to olive oil bolus (Figure 8A, lane 2 and 4). In contrast to ATGL, intestinal expression of other proteins including HSL, pHSL (a phosphorylated HSL at serine 563 by Phosphokinase A), MTP, and ARFRP1 was not affected by Grasp55 deficiency, and expression of ARFRP1, pHSL, and HSL was normally increased by exogenous lipid (Figure 8A) (quantification shown in Figure 8B).

To further investigate the mechanism how the intestinal expression of ATGL was decreased by the depletion of Grasp55, we examined the characteristics of ATGL by using the Grasp55 knockdown Caco-2 stable cells. We found that GRASP55 depletion decreased the total levels of ATGL in Caco-2 cells (Figure 8C, lane 1 and 3) by a process that was sensitive to a proteasomal inhibitor MG132 (Figure 8C, lane 3 and 4).

However, there was no difference in the expression of GBF1 and ARF1 (Figure 8C). Therefore, impaired delivery of ATGL to LDs resulted in its degradation by the proteasome (quantification shown in Figure 8D).

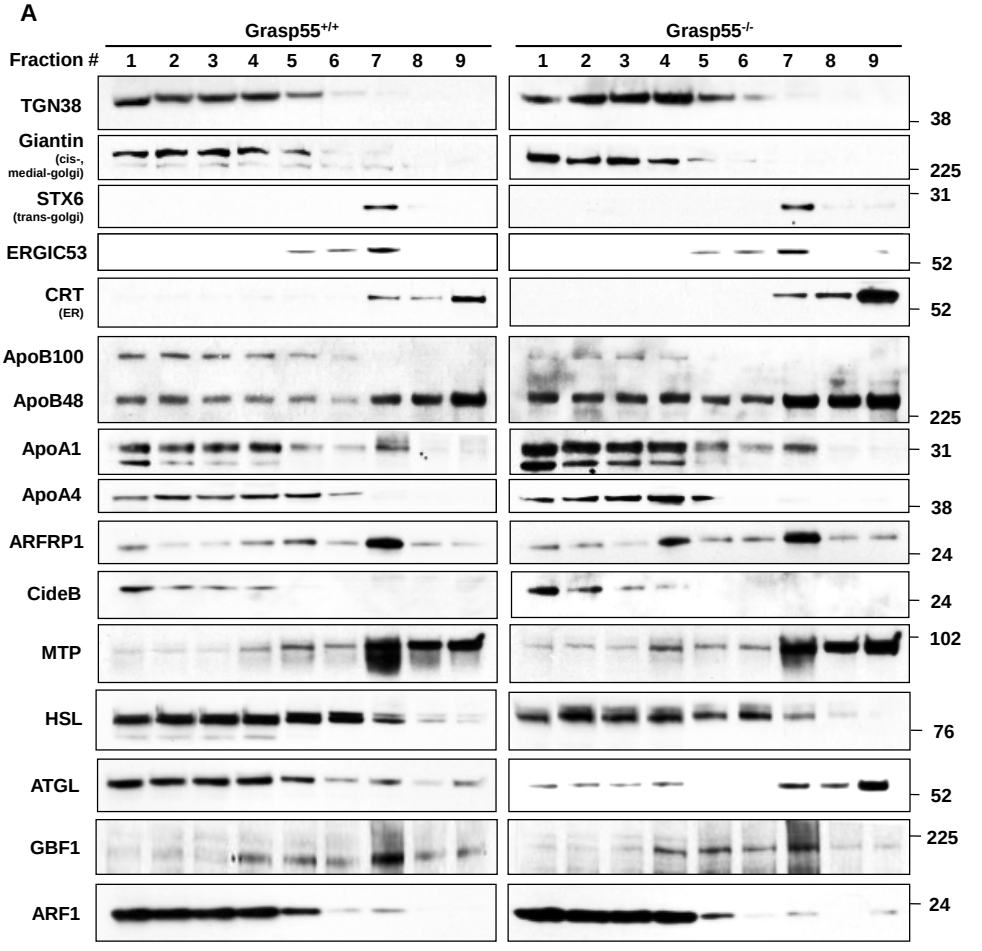

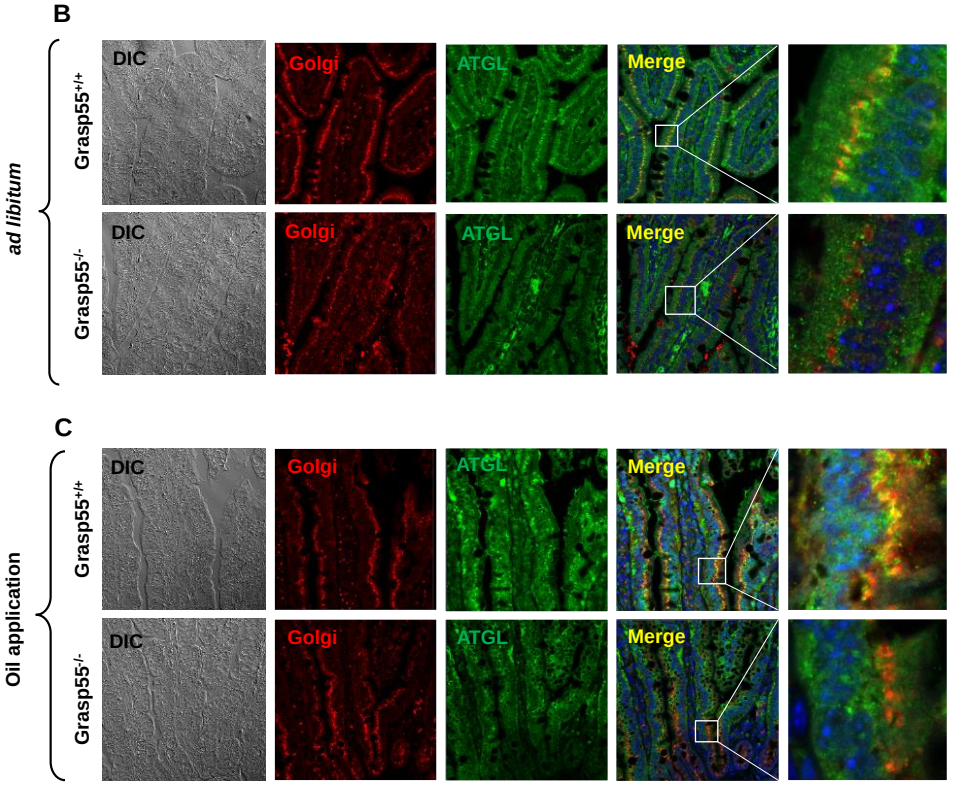

Figure 7. Depletion of Grasp55 affects the cellular localization of ATGL. (A) Membrane fractions of intestinal epithelial cells in Grasp55$^{+/+}$ and Grasp55$^{-/-}$ mice fed with normal diet were prepared by density gradient ultracentrifugation using an OptiPrep^{TM} gradient followed by immunoblotting with the indicated antibodies. Organellar markers: TGN38 (the trans-Golgi network), Giantin (the cis-/medial-Golgi), STX6 (the trans-Golgi), ERGIC53 (the ER-Golgi intermediate compartment), and Calreticulin (the ER). **(B and C)** Cellular localization of ATGL was examined in intestinal epithelium in Grasp55$^{+/+}$ and Grasp55$^{-/-}$ mice which were free to food **(B)** or after olive oil bolus **(C)**. Intestinal tissues were co-stained for ATGL and the Golgi marker protein GM130. Images acquisition for all was performed with the same settings.

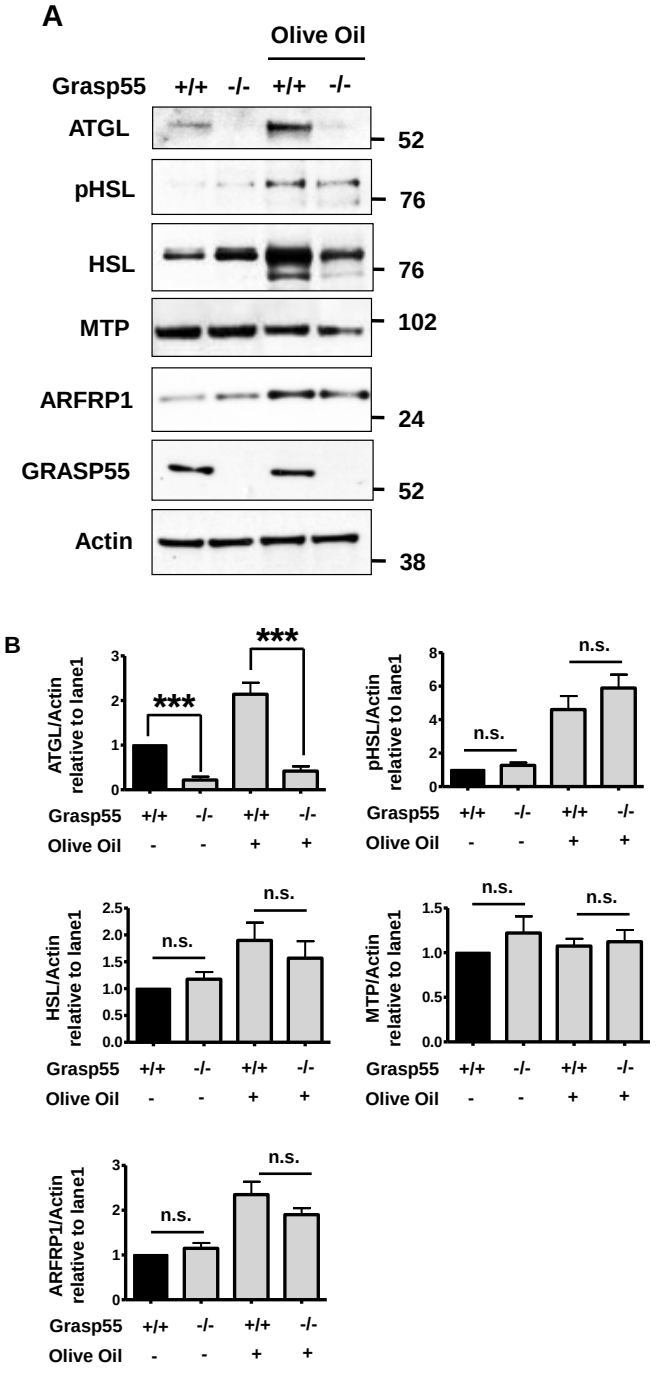

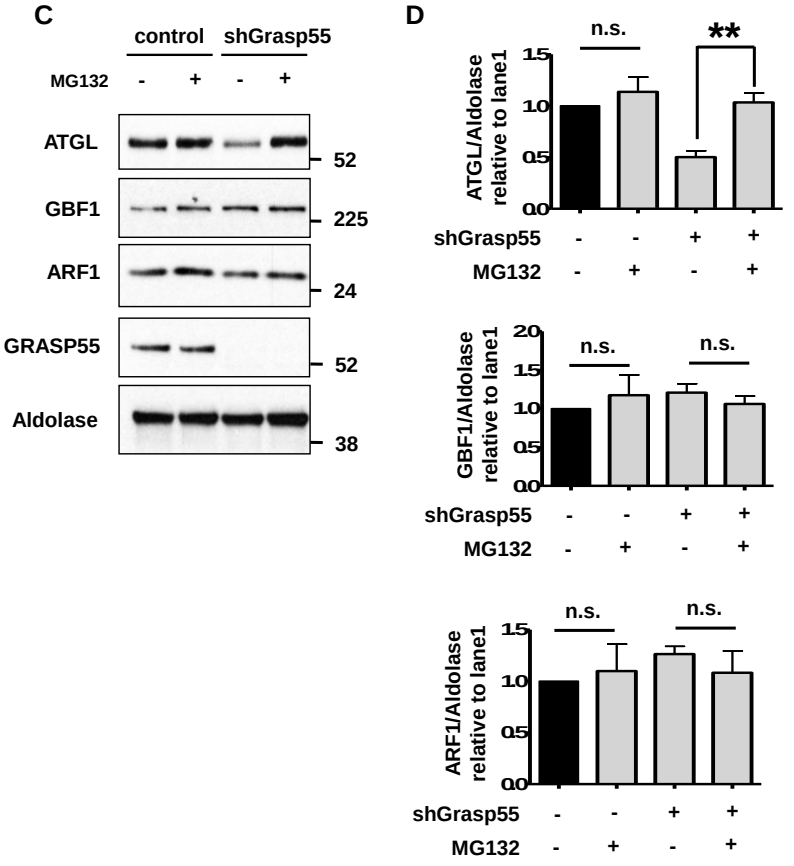

Figure 8. Depletion of Grasp55 decreases the protein expression and stability of ATGL. (A) Intestinal protein expression of 16hr fasted Grasp55$^{+/+}$ and Grasp55$^{-/-}$ mice (lane 1 and 2) or of mice 4hr after receiving an oil bolus (lane 3 and 4) was analyzed by western blotting with the indicated antibodies (n=6). The level of actin was monitored as a loading control. The results of multiple experiments are summarized in **(B)**. **(C)** Immunoblot analysis of ATGL, GBF1 and ARF1 expression in the absence or presence of a proteasomal inhibitor MG132 with Caco-2 control cell and stable cell of which Grasp55 expression was stably suppressed. The level of aldolase was monitored as a loading control. The results of multiple experiments are summarized in **(D).** Data shown are mean±SEM (*p<0.05, **p<0.01, ***p<0.001, n.s., not significant).

6. Grasp55$^{-/-}$ mice has a defect of targeting ATGL into lipid droplets

To investigate whether the decrease in protein expression of ATGL also affects its incorporation into LDs, we conducted immunohistochemistry with ATGL and adipose differentiation-related protein (ADRP), one of the LD-associated proteins. In control mice, LDs were dramatically induced by oil application and co-localization between ATGL and ADRP was found around LD (Figure 9B, Grasp55$^{+/+}$) when compared to the condition of normal diet (Figure 9A, Grasp55$^{+/+}$). However, the deficiency of Grasp55 significantly diminished the co-localization of ATGL with the LD marker ADRP (Figure 9B, Grasp55$^{-/-}$). These findings that the targeting of ATGL into LDs was impaired by depletion of Grasp55 were also reaffirmed *in vitro* system. ATGL localized around the LDs in control Caco-2 while knock-down of Grasp55 inhibited the lipid-induced localization of ATGL into LDs (Figure 9C).

Next, in order to investigate the cause of the decrease of ATGL targeting into LDs by Grasp55 depletion, we examined whether loss of Grasp55 causes the structural problem of the Golgi because one of the main roles of Grasp55 is to maintain the structure of the Golgi. On electron microscopy, the intestinal Golgi of Grasp55$^{-/-}$ mice was not sufficiently stacked compared to the control (Figure 10A, left panel). After oral gavage of olive oil, the Golgi of the Grasp55$^{-/-}$ mice still showed a loose appearance (Figure 10A, right panel). To investigate the structure of the Golgi in a functional manner, we performed fluorescence recovery after photobleaching (FRAP). Since this assay was impossible with tissue, we used mouse epithelial fibroblasts (MEFs) which were transfected with the enhanced yellow fluorescent protein (pEYFP)-Golgi[75]. It was found that 50% recovery of photobleached EYFP-Golgi in Grasp55$^{+/+}$ MEFs which localizes to medial- and trans-Golgi took about 150sec after bleaching, but EYFP-Golgi in Grasp55$^{-/-}$ MEFs recovered slowly and incompletely (about 40% of the original fluorescence after 500 seconds) (Figure 10C and 10D). These results demonstrated that the Golgi was functionally unlinked at the medial- or trans- side by depletion of Grasp55.

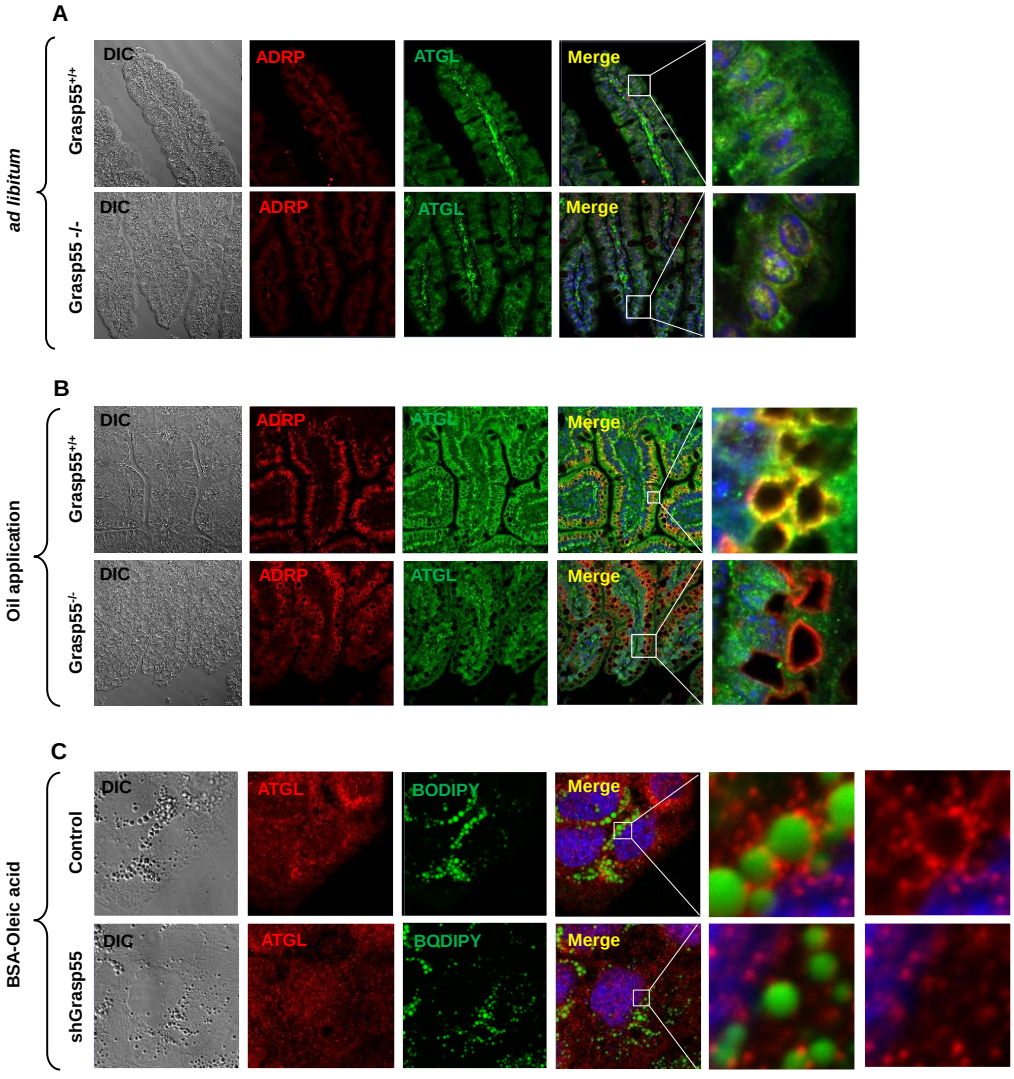

Figure 9. Grasp55 deficiency causes a defect of targeting ATGL into lipid droplets. (A and B) Subcellular localization of ATGL was examined in intestinal epithelium of mice which was co-immunostained with antibodies against ATGL and ADRP after normal diet **(A)** or olive oil bolus **(B)**. **(C)** Caco-2 cells were stained with BODIPY 493/503 and an anti-ATGL antibody in the presence of 400 μM oleic acid for 16hr. Images acquisition for all was performed with the same settings.

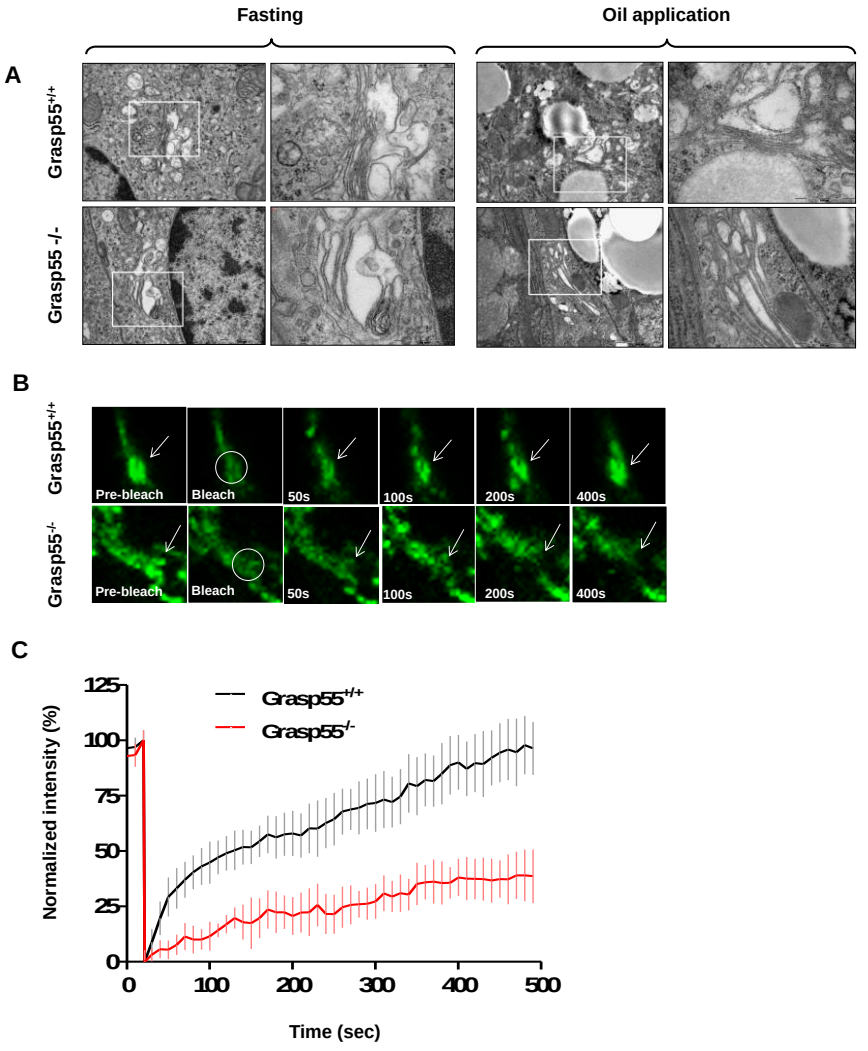

Figure 10. The Golgi appears abnormal in intestine from Grasp55$^{-/-}$ mice. (A) Ultrastructural analysis of the Golgi in Grasp55$^{+/+}$ and Grasp55$^{-/-}$ mice with 16hr fasted or 4hr after receiving an oil bolus. **(B)** Fluorescence recovery after photobleaching (FRAP) on MEFs of Grasp55$^{+/+}$ and Grasp55$^{-/-}$ mice. Time course of the Golgi fluorescence recovery after photo-bleaching of EYFP-Golgi protein. White circles encompass the photo-bleached region. Arrows point to bleached regions. **(C)** Fluorescence levels in bleached region was measured and was plotted versus time (n=10 cells, mean±SEM). The graph (C) corresponds to panel (B).

IV. DISCUSSION

Most of the exogenous lipids are absorbed in the small intestine and are packed into the core of the chylomicron. The chylomicron is a unique lipid carrier synthesized only in the small intestine. It has been found that the defect of synthesis and secretion of chylomicron results in lipid accumulation in the small intestinal epithelium and systemic lipid imbalance using genetic knockout mice models[65]. The major proteins regulating the physiological function of chylomicron are apolipoproteins and molecular mechanisms how apolipoproteins synthesized in the ER are incorporated to chylomicron have been actively studied. In particular, ER-to-Golgi transport of the pre-chylomicron transport vesicle (PCTV), a pre-mature form budged-out in the ER, has been intensively studied. As a result, Sar1b, Sec24C, Sec13/31, Syntaxin5, Vti1a, VAMP7 and PKCζ have been identified as the major molecular players[3,76-81]. However, it is still elusive as to how PCTV reached the Golgi matures into chylomicrons which are secreted from the intestinal epithelial cells into the lymphatic system.

In the postprandial period, when the supply of lipids from the outside is interrupted, the epithelial cells of the small intestine can still secrete chylomicron. This is because enterocytes store absorbed lipids in the form of LDs and utilize LDs as a reservoir of lipids. This cross-talk between LDs and chylomicron contribute to maintaining lipid homeostasis by moderating the postprandial plasma lipid concentration curve[29]. The present results indicate that GRASP55 is a novel regulator involved in the cross-talk of LDs and chylomicrons. It has been demonstrated that the Golgi protein is involved in lipid transport. Interestingly, one review paper has provided a new insight into the direct function of the Golgi in lipid transport by comparing the maturation process of chylomicron with modification of lipid particles[82]. In particular, a recent research using *Drosophila* has revealed that GRASP is the energy sensing molecule that regulates the unconventional secretion of Upd2, an orthologue of mammalian leptin, in response to nutritional status[83]. However,

unlike the mammalian GRASP, *Drosophila* GRASP was broadly present in intra-cellular compartments including the periphery of LDs, cytosol, plasma membrane and the Golgi. This suggests that the mammalian GRASP has been exclusively resident in the Golgi, which might allow the mammalian Golgi to be involved in the regulation of cellular lipid.

Recently, LDs have become increasingly important as they are found to be closely related to various human diseases such as obesity, diabetes and atherosclerosis[84]. A number of studies on the life cycle of LDs such as their origin, formation, and regulation have been actively conducted[56,57]. Nevertheless, there is still debate about the origin of LDs. The traditional hypothesis for the origins of LDs is that LDs are synthesized from the cytoplasmic leaflet of the ER membrane. The empirical evidence for this are the ER-to LD bridge[42] and a wide range of common denominators between LD-associated proteins and the ER proteins identified through large-scale proteomics[30-38]. However, since evidence has been revealed that LDs are not entirely dependent on the ER, the functional range of LDs has greatly increased. For example, the detailed comparison of the composition of the phospholipids between the LD membrane and the ER membrane revealed that there were unexpectedly many inconsistent components[54]. In addition, Soni *et al.* suggested that LDs originated from ERGIC by presenting evidences of immuocytochemistry and electron tomography which demonstrated the co-localization of p58 (which localizes to ERGIC) with TIP47 . In order to accurately elucidate the origins of LDs, it is necessary to obtain technical capability to isolate LDs with the high purity and to closely observe trafficking of LD-associated proteins.

The morphological and functional complexity of LDs has been greatly expanded as the size and intracellular location of LDs are known to be highly heterogeneous[56]. The complexity of these LDs is due to the structural specificity of the intracellular organelles, which is surrounded only by the phospholipid monolayer, allowing them to interact in a unique way with various organelles in the cell. In particular, numerous proteins on the LD surface suggest functional complexity of LDs. Interestingly, membrane trafficking proteins were commonly identified from multiple proteomics

results, including Rab11A, Rab1A, Rab1B, and Rab18, which are known to exist in the Golgi[85-88]. This is an interesting result in that the Golgi has a potential possibility of interacting with LDs through the trafficking machinery. The results of this study suggest more direct evidences that the Golgi is involved in LD biogenesis. Knockout mice lacking Grasp55, one of the major regulatory proteins located in the Golgi, showed a lipid deficiency phenotype (Figure 2A, 2B, Table 1 and Table 2). This phenomenon was also maintained in high-fat diet (Figure 2C-E). There was no abnormality in the absorption of amino acids (Figure 4D-F). The small intestine of Grasp55$^{-/-}$ mice has been shown to be impaired in lipid absorption (Figure 3B and 4A). These results were reproduced through an *in vitro* system using differentiated Caco-2 cells (Figure 4C). Grasp55$^{-/-}$ mice showed a significant decrease in secretion (Figure 5A and 5D). Especially, the intestinal epithelial cells of Grasp55$^{-/-}$ had a reduced number of larger chylomicrons in compare to control chylomicrons, indicating that the chylomicron of Grasp55$^{-/-}$ showed intestinal retention phenotype (Figure 5B).

In addition, the supersized LDs were observed in the intestine of Grasp55$^{-/-}$ mice after oral gavage of excess lipid and when sufficient time was given for the lipid to be absorbed into the body, but not in control mice (Figure 6D and 6E). Surprisingly, the supersized LDs by the depletion of Grasp55 were caused by the defect of targeting of ATGL into LDs (Figure 9B and 9C). However, there were no changes in intestinal cellular location and protein expression of other proteins including apolipoproteins, MTP, HSL, ARFRP1 and CIDEB (Figure 6A-C, 6F, 7A and 8A). The deficiency of Grasp55 reduced the co-localization between ATGL and the Golgi (Figure 7A and 7B). It is directly indicated that the trafficking pathway of ATGL includes not only the ER and the ERGIC but also the Golgi. Interestingly, it is known that delivery of ATGL to LD is dependent on COPI[43]. COPI vesicles are involved in retrograde transport of ER-to-Golgi[1], anterograde transport of ERGIC-to-Golgi[89,90] and anterograde intra-Golgi transport[91]. Therefore, it is plausible that COPI knock-down may suppress targeting of ATGL to LD through inhibiting the trafficking to the Golgi or in the Golgi. In particular, co-localization of ATGL with the Golgi was significantly increased (Figure 7C) when the expression level of ATGL was increased by lipid (Figure 8A, lane 1 and

3). These results indicate that the intracellular migration of ATGL is activated to compensate for the loss of lipid homeostatic balance by absorbing excess external lipids, resulting in increased transport to the Golgi[92]. However, since the enhanced co-localization were not reproduced in Grasp55$^{-/-}$ intestinal epithelial cells (Figure 7C), GRASP55 seems to be also essential for the transport of lipid-induced ATGL. In addition, ATGL, which failed to reach LDs by deficiency of Grasp55, was decreased through proteasomal degradation (Figure 8C). This result was consistent with the previous report[43].

The mechanisms for targeting of LD-associated proteins have been recently reported. Although there are relatively well-defined proteins in the targeting mechanism, the mechanisms for most LD proteins are still unknown[57]. A notable finding of this present study is that the Golgi protein plays a critical role in the targeting of LD-associated protein such as ATGL into LDs which are important for providing chylomicron with lipid sources. In the previous *in vivo* studies, the whole body knock-out mice of ATGL (ATGL KO) showed decreased survival rate, increased body weight, increased fat mass, and increased adipose tissue due to decreased lipolysis of the whole body[93]. In particular, ATGL KO showed TG accumulation in myocardial cells, increased concentric left-ventricular hypertrophy and impairment of left ventricular systolic function. In conditional ATGL knock-out mice which lack ATGL exclusively in the intestine (ATGLiKO)[73], it has been reported that intestinal lipid was dramatically accumulated and intestinal lipase activity was decreased, similar to phenotypes of Grasp55$^{-/-}$ mice (Figure 3B). However, unlike Grasp55$^{-/-}$ mice, ATGLiKO showed no change in TG absorption by systemic circulation. To elucidate why these phenotypic differences occur, more detailed studies of the intracellular trafficking and function of ATGL are needed.

A remaining question is how GRASP55 facilitates the targeting of ATGL into LDs. Ultrastructural analysis of the Golgi and FRAP on MEFs suggest that the structural and functional defects of the Golgi are the underlying cause for phenotypes of Grasp55$^{-/-}$ mice (Figure 10A and 10B). However, further study is needed to investigate whether ATGL directly correlates with GRASP55. Interestingly, it was

found that ATGL did not dissolve even under harsh extraction conditions using Triton X-100 or urea, despite the absence of the transmembrane domain[43]. This characteristic suggests that ATGL has some unidentified structural uniqueness.

V. CONCLUSION

The Golgi complex plays a pivotal role in transporting cellular proteins and lipids. We have studied the novel role of the Golgi in lipid transport using an *in vivo* murine model lacking Grasp55, one of the Golgi-resident proteins. Grasp55$^{-/-}$ mice had growth retardation, reduced adipose tissues and reduced plasma lipid levels. The significant reduction of body fat in Grasp55$^{-/-}$ mice was attributed to the defect of intestinal lipid uptake. In particular, deficiency of Grasp55 induced the formation of supersized intestinal LDs. These results were caused by changes in cellular localization and protein stability of ATGL which is one of LD-associated lipases and plays a crucial role in lipolysis of LDs. Taken together, the current investigation indicates that GRASP55 is a new regulator of lipid droplets and is responsible for secretion of chylomicron, and that the Golgi protein is involved in cross-talk between chylomicron and LD. These results also provide new mechanistic insights into the pathogenesis and therapeutics of LD-associated diseases.

REFERENCES

1. Schekman R, Orci L. Coat proteins and vesicle budding. Science 1996;271:1526-33.
2. Bonifacino JS, Glick BS. The mechanisms of vesicle budding and fusion. Cell 2004;116:153-66.
3. Wong DM, Webb JP, Malinowski PM, Xu E, Macri J, Adeli K. Proteomic profiling of intestinal prechylomicron transport vesicle (PCTV)-associated proteins in an animal model of insulin resistance (94 char). J Proteomics 2010;73:1291-305.
4. Lee MC, Miller EA, Goldberg J, Orci L, Schekman R. Bi-directional protein transport between the ER and Golgi. Annu Rev Cell Dev Biol 2004;20:87-123.
5. Viotti C. ER to Golgi-Dependent Protein Secretion: The Conventional Pathway. Methods Mol Biol 2016;1459:3-29.
6. Duncan R, Richardson SC. Endocytosis and intracellular trafficking as gateways for nanomedicine delivery: opportunities and challenges. Mol Pharm 2012;9:2380-402.
7. Farquhar MG, Palade GE. The Golgi apparatus: 100 years of progress and controversy. Trends Cell Biol 1998;8:2-10.
8. Roth MG. Lipid regulators of membrane traffic through the Golgi complex. Trends Cell Biol 1999;9:174-9.
9. Wilson C, Venditti R, Rega LR, Colanzi A, D'Angelo G, De Matteis MA. The Golgi apparatus: an organelle with multiple complex functions. Biochem J 2011;433:1-9.
10. Lowe M. Structural organization of the Golgi apparatus. Curr Opin Cell Biol 2011;23:85-93.
11. Gomez-Navarro N, Miller E. Protein sorting at the ER-Golgi interface. J Cell Biol 2016;215:769-78.
12. Guo Y, Sirkis DW, Schekman R. Protein sorting at the trans-Golgi network.

Annu Rev Cell Dev Biol 2014;30:169-206.

13. Barr FA, Puype M, Vandekerckhove J, Warren G. GRASP65, a protein involved in the stacking of Golgi cisternae. Cell 1997;91:253-62.
14. Shorter J, Watson R, Giannakou ME, Clarke M, Warren G, Barr FA. GRASP55, a second mammalian GRASP protein involved in the stacking of Golgi cisternae in a cell-free system. EMBO J 1999;18:4949-60.
15. Zhang X, Wang Y. GRASPs in Golgi Structure and Function. Front Cell Dev Biol 2015;3:84.
16. Ladinsky MS, Mastronarde DN, McIntosh JR, Howell KE, Staehelin LA. Golgi structure in three dimensions: functional insights from the normal rat kidney cell. J Cell Biol 1999;144:1135-49.
17. Jarvela T, Linstedt AD. Isoform-specific tethering links the Golgi ribbon to maintain compartmentalization. Mol Biol Cell 2014;25:133-44.
18. Xiang Y, Wang Y. GRASP55 and GRASP65 play complementary and essential roles in Golgi cisternal stacking. J Cell Biol 2010;188:237-51.
19. Xiang Y, Zhang X, Nix DB, Katoh T, Aoki K, Tiemeyer M, et al. Regulation of protein glycosylation and sorting by the Golgi matrix proteins GRASP55/65. Nat Commun 2013;4:1659.
20. Giuliani F, Grieve A, Rabouille C. Unconventional secretion: a stress on GRASP. Curr Opin Cell Biol 2011;23:498-504.
21. Kinseth MA, Anjard C, Fuller D, Guizzunti G, Loomis WF, Malhotra V. The Golgi-associated protein GRASP is required for unconventional protein secretion during development. Cell 2007;130:524-34.
22. Malhotra V. Unconventional protein secretion: an evolving mechanism. EMBO J 2013;32:1660-4.
23. Schotman H, Karhinen L, Rabouille C. dGRASP-mediated noncanonical integrin secretion is required for Drosophila epithelial remodeling. Dev Cell 2008;14:171-82.
24. Gee HY, Noh SH, Tang BL, Kim KH, Lee MG. Rescue of DeltaF508-CFTR trafficking via a GRASP-dependent unconventional secretion pathway. Cell

2011;146:746-60.

25. Cleyrat C, Darehshouri A, Steinkamp MP, Vilaine M, Boassa D, Ellisman MH, et al. Mpl traffics to the cell surface through conventional and unconventional routes. Traffic 2014;15:961-82.

26. Valentine CD, Lukacs GL, Verkman AS, Haggie PM. Reduced PDZ interactions of rescued DeltaF508CFTR increases its cell surface mobility. J Biol Chem 2012;287:43630-8.

27. Levi SK, Glick BS. GRASPing unconventional secretion. Cell 2007;130:407-9.

28. Prinz WA. Lipid trafficking sans vesicles: where, why, how? Cell 2010;143:870-4.

29. Beilstein F, Carriere V, Leturque A, Demignot S. Characteristics and functions of lipid droplets and associated proteins in enterocytes. Exp Cell Res 2016;340:172-9.

30. Bouchoux J, Beilstein F, Pauquai T, Guerrera IC, Chateau D, Ly N, et al. The proteome of cytosolic lipid droplets isolated from differentiated Caco-2/TC7 enterocytes reveals cell-specific characteristics. Biol Cell 2011;103:499-517.

31. Cermelli S, Guo Y, Gross SP, Welte MA. The lipid-droplet proteome reveals that droplets are a protein-storage depot. Curr Biol 2006;16:1783-95.

32. Brasaemle DL, Dolios G, Shapiro L, Wang R. Proteomic analysis of proteins associated with lipid droplets of basal and lipolytically stimulated 3T3-L1 adipocytes. J Biol Chem 2004;279:46835-42.

33. D'Aquila T, Sirohi D, Grabowski JM, Hedrick VE, Paul LN, Greenberg AS, et al. Characterization of the proteome of cytoplasmic lipid droplets in mouse enterocytes after a dietary fat challenge. PLoS One 2015;10:e0126823.

34. Ding Y, Yang L, Zhang S, Wang Y, Du Y, Pu J, et al. Identification of the major functional proteins of prokaryotic lipid droplets. J Lipid Res 2012;53:399-411.

35. Krahmer N, Hilger M, Kory N, Wilfling F, Stoehr G, Mann M, et al. Protein correlation profiles identify lipid droplet proteins with high confidence. Mol

Cell Proteomics 2013;12:1115-26.

36. Zhang P, Na H, Liu Z, Zhang S, Xue P, Chen Y, et al. Proteomic study and marker protein identification of Caenorhabditis elegans lipid droplets. Mol Cell Proteomics 2012;11:317-28.

37. Currie E, Guo X, Christiano R, Chitraju C, Kory N, Harrison K, et al. High confidence proteomic analysis of yeast LDs identifies additional droplet proteins and reveals connections to dolichol synthesis and sterol acetylation. J Lipid Res 2014;55:1465-77.

38. Fujimoto Y, Itabe H, Sakai J, Makita M, Noda J, Mori M, et al. Identification of major proteins in the lipid droplet-enriched fraction isolated from the human hepatocyte cell line HuH7. Biochim Biophys Acta 2004;1644:47-59.

39. Robenek H, Hofnagel O, Buers I, Robenek MJ, Troyer D, Severs NJ. Adipophilin-enriched domains in the ER membrane are sites of lipid droplet biogenesis. J Cell Sci 2006;119:4215-24.

40. Zehmer JK, Bartz R, Bisel B, Liu P, Seemann J, Anderson RG. Targeting sequences of UBXD8 and AAM-B reveal that the ER has a direct role in the emergence and regression of lipid droplets. J Cell Sci 2009;122:3694-702.

41. Lingwood D, Simons K. Lipid rafts as a membrane-organizing principle. Science 2010;327:46-50.

42. Wilfling F, Wang H, Haas JT, Krahmer N, Gould TJ, Uchida A, et al. Triacylglycerol synthesis enzymes mediate lipid droplet growth by relocalizing from the ER to lipid droplets. Dev Cell 2013;24:384-99.

43. Soni KG, Mardones GA, Sougrat R, Smirnova E, Jackson CL, Bonifacino JS. Coatomer-dependent protein delivery to lipid droplets. J Cell Sci 2009;122:1834-41.

44. Hesse D, Radloff K, Jaschke A, Lagerpusch M, Chung B, Tailleux A, et al. Hepatic trans-Golgi action coordinated by the GTPase ARFRP1 is crucial for lipoprotein lipidation and assembly. J Lipid Res 2014;55:41-52.

45. Hommel A, Hesse D, Volker W, Jaschke A, Moser M, Engel T, et al. The ARF-like GTPase ARFRP1 is essential for lipid droplet growth and is

involved in the regulation of lipolysis. Mol Cell Biol 2010;30:1231-42.

46. Almahbobi G, Williams LJ, Han XG, Hall PF. Binding of lipid droplets and mitochondria to intermediate filaments in rat Leydig cells. J Reprod Fertil 1993;98:209-17.

47. Stone SJ, Levin MC, Zhou P, Han J, Walther TC, Farese RV, Jr. The endoplasmic reticulum enzyme DGAT2 is found in mitochondria-associated membranes and has a mitochondrial targeting signal that promotes its association with mitochondria. J Biol Chem 2009;284:5352-61.

48. Murphy S, Martin S, Parton RG. Lipid droplet-organelle interactions; sharing the fats. Biochim Biophys Acta 2009;1791:441-7.

49. Binns D, Januszewski T, Chen Y, Hill J, Markin VS, Zhao Y, et al. An intimate collaboration between peroxisomes and lipid bodies. J Cell Biol 2006;173:719-31.

50. Liu P, Bartz R, Zehmer JK, Ying YS, Zhu M, Serrero G, et al. Rab-regulated interaction of early endosomes with lipid droplets. Biochim Biophys Acta 2007;1773:784-93.

51. Kaushik S, Cuervo AM. Degradation of lipid droplet-associated proteins by chaperone-mediated autophagy facilitates lipolysis. Nat Cell Biol 2015;17:759-70.

52. Dvorak AM, Morgan ES, Weller PF. RNA is closely associated with human mast cell lipid bodies. Histol Histopathol 2003;18:943-68.

53. Targett-Adams P, Boulant S, McLauchlan J. Visualization of double-stranded RNA in cells supporting hepatitis C virus RNA replication. J Virol 2008;82:2182-95.

54. Tauchi-Sato K, Ozeki S, Houjou T, Taguchi R, Fujimoto T. The surface of lipid droplets is a phospholipid monolayer with a unique Fatty Acid composition. J Biol Chem 2002;277:44507-12.

55. Beller M, Thiel K, Thul PJ, Jackle H. Lipid droplets: a dynamic organelle moves into focus. FEBS Lett 2010;584:2176-82.

56. Thiam AR, Beller M. The why, when and how of lipid droplet diversity. J Cell

Sci 2017;130:315-24.

57. Kory N, Farese RV, Jr., Walther TC. Targeting Fat: Mechanisms of Protein Localization to Lipid Droplets. Trends Cell Biol 2016;26:535-46.

58. Tansey JT, Sztalryd C, Gruia-Gray J, Roush DL, Zee JV, Gavrilova O, et al. Perilipin ablation results in a lean mouse with aberrant adipocyte lipolysis, enhanced leptin production, and resistance to diet-induced obesity. Proc Natl Acad Sci U S A 2001;98:6494-9.

59. Thiam AR, Farese RV, Jr., Walther TC. The biophysics and cell biology of lipid droplets. Nat Rev Mol Cell Biol 2013;14:775-86.

60. Gao Q, Goodman JM. The lipid droplet-a well-connected organelle. Front Cell Dev Biol 2015;3:49.

61. Drin G. Topological regulation of lipid balance in cells. Annu Rev Biochem 2014;83:51-77.

62. Kim J, Noh SH, Piao H, Kim DH, Kim K, Cha JS, et al. Monomerization and ER Relocalization of GRASP Is a Requisite for Unconventional Secretion of CFTR. Traffic 2016;17:733-53.

63. Qiu B, Simon MC. BODIPY 493/503 Staining of Neutral Lipid Droplets for Microscopy and Quantification by Flow Cytometry. Bio Protoc 2016;6.

64. Singer D, Camargo SM, Ramadan T, Schafer M, Mariotta L, Herzog B, et al. Defective intestinal amino acid absorption in Ace2 null mice. Am J Physiol Gastrointest Liver Physiol 2012;303:G686-95.

65. Durkin ME, Qian X, Popescu NC, Lowy DR. Isolation of Mouse Embryo Fibroblasts. Bio Protoc 2013;3.

66. Chau YY, Bandiera R, Serrels A, Martinez-Estrada OM, Qing W, Lee M, et al. Visceral and subcutaneous fat have different origins and evidence supports a mesothelial source. Nat Cell Biol 2014;16:367-75.

67. Mansbach CM, Siddiqi SA. The biogenesis of chylomicrons. Annu Rev Physiol 2010;72:315-33.

68. van Greevenbroek MM, de Bruin TW. Chylomicron synthesis by intestinal cells in vitro and in vivo. Atherosclerosis 1998;141 Suppl 1:S9-16.

69. Jaschke A, Chung B, Hesse D, Kluge R, Zahn C, Moser M, et al. The GTPase ARFRP1 controls the lipidation of chylomicrons in the Golgi of the intestinal epithelium. Hum Mol Genet 2012;21:3128-42.

70. Zhang LJ, Wang C, Yuan Y, Wang H, Wu J, Liu F, et al. Cideb facilitates the lipidation of chylomicrons in the small intestine. J Lipid Res 2014;55:1279-87.

71. Demignot S, Beilstein F, Morel E. Triglyceride-rich lipoproteins and cytosolic lipid droplets in enterocytes: key players in intestinal physiology and metabolic disorders. Biochimie 2014;96:48-55.

72. Wang S, Soni KG, Semache M, Casavant S, Fortier M, Pan L, et al. Lipolysis and the integrated physiology of lipid energy metabolism. Mol Genet Metab 2008;95:117-26.

73. Obrowsky S, Chandak PG, Patankar JV, Povoden S, Schlager S, Kershaw EE, et al. Adipose triglyceride lipase is a TG hydrolase of the small intestine and regulates intestinal PPARalpha signaling. J Lipid Res 2013;54:425-35.

74. Ellong EN, Soni KG, Bui QT, Sougrat R, Golinelli-Cohen MP, Jackson CL. Interaction between the triglyceride lipase ATGL and the Arf1 activator GBF1. PLoS One 2011;6:e21889.

75. Watzele G, Berger EG. Near identity of HeLa cell galactosyltransferase with the human placental enzyme. Nucleic Acids Res 1990;18:7174.

76. Siddiqi SA, Gorelick FS, Mahan JT, Mansbach CM, 2nd. COPII proteins are required for Golgi fusion but not for endoplasmic reticulum budding of the pre-chylomicron transport vesicle. J Cell Sci 2003;116:415-27.

77. Jones B, Jones EL, Bonney SA, Patel HN, Mensenkamp AR, Eichenbaum-Voline S, et al. Mutations in a Sar1 GTPase of COPII vesicles are associated with lipid absorption disorders. Nat Genet 2003;34:29-31.

78. Siddiqi SA, Siddiqi S, Mahan J, Peggs K, Gorelick FS, Mansbach CM, 2nd. The identification of a novel endoplasmic reticulum to Golgi SNARE complex used by the prechylomicron transport vesicle. J Biol Chem 2006;281:20974-82.

79. Siddiqi SA, Mansbach CM, 2nd. PKC zeta-mediated phosphorylation controls budding of the pre-chylomicron transport vesicle. J Cell Sci 2008;121:2327-38.
80. Siddiqi S, Siddiqi SA, Mansbach CM, 2nd. Sec24C is required for docking the prechylomicron transport vesicle with the Golgi. J Lipid Res 2010;51:1093-100.
81. Siddiqi S, Saleem U, Abumrad NA, Davidson NO, Storch J, Siddiqi SA, et al. A novel multiprotein complex is required to generate the prechylomicron transport vesicle from intestinal ER. J Lipid Res 2010;51:1918-28.
82. Hesse D, Jaschke A, Chung B, Schurmann A. Trans-Golgi proteins participate in the control of lipid droplet and chylomicron formation. Biosci Rep 2013;33:1-9.
83. Rajan A, Housden BE, Wirtz-Peitz F, Holderbaum L, Perrimon N. A Mechanism Coupling Systemic Energy Sensing to Adipokine Secretion. Dev Cell 2017;43:83-98 e6.
84. Onal G, Kutlu O, Gozuacik D, Dokmeci Emre S. Lipid Droplets in Health and Disease. Lipids Health Dis 2017;16:128.
85. Bartz R, Li WH, Venables B, Zehmer JK, Roth MR, Welti R, et al. Lipidomics reveals that adiposomes store ether lipids and mediate phospholipid traffic. J Lipid Res 2007;48:837-47.
86. Liu P, Ying Y, Zhao Y, Mundy DI, Zhu M, Anderson RG. Chinese hamster ovary K2 cell lipid droplets appear to be metabolic organelles involved in membrane traffic. J Biol Chem 2004;279:3787-92.
87. Wan HC, Melo RC, Jin Z, Dvorak AM, Weller PF. Roles and origins of leukocyte lipid bodies: proteomic and ultrastructural studies. FASEB J 2007;21:167-78.
88. Umlauf E, Csaszar E, Moertelmaier M, Schuetz GJ, Parton RG, Prohaska R. Association of stomatin with lipid bodies. J Biol Chem 2004;279:23699-709.
89. Cosson P, Letourneur F. Coatomer (COPI)-coated vesicles: role in intracellular transport and protein sorting. Curr Opin Cell Biol 1997;9:484-7.

90. Appenzeller-Herzog C, Hauri HP. The ER-Golgi intermediate compartment (ERGIC): in search of its identity and function. J Cell Sci 2006;119:2173-83.

91. Rabouille C, Klumperman J. Opinion: The maturing role of COPI vesicles in intra-Golgi transport. Nat Rev Mol Cell Biol 2005;6:812-7.

92. Farese RV, Jr., Ruland SL, Flynn LM, Stokowski RP, Young SG. Knockout of the mouse apolipoprotein B gene results in embryonic lethality in homozygotes and protection against diet-induced hypercholesterolemia in heterozygotes. Proc Natl Acad Sci U S A 1995;92:1774-8.

93. Haemmerle G, Lass A, Zimmermann R, Gorkiewicz G, Meyer C, Rozman J, et al. Defective lipolysis and altered energy metabolism in mice lacking adipose triglyceride lipase. Science 2006;312:734-7.

ABSTRACT (IN KOREAN)

지질 수송에 대한 GRASP55 단백의 생리학적 역할

<지도교수 이 민 구>

연세대학교 대학원 의과학과

김지윤

Golgi 는 세포 내의 단백 및 지질 수송에 핵심적인 역할을 수행한다. 이러한 Golgi 의 기능은 다양한 종류의 조절 단백들의 정밀한 작용에 의해서 유지된다. 지금까지 Golgi 에 대한 연구는 단백 수송에 집중되어 진행하여 왔다. 하지만 세포 내 지질 수송, 특히 중성 지방 수송에 대한 연구는 많이 부족하다. 본 연구에서는 Golgi 를 구성하는 주요 단백 중 하나인 GRASP55 가 결여되어 있는 마우스를 이용하여 GRASP55 가 중성 지방 분해 효소 (ATGL)의 장내 지방 방울 (lipid droplet)로의 이동을 조절함으로써 킬로마이크론 (chylomicron)의 형성에 핵심적인 역할을 수행함을 규명하였다. 이러한 연구 결과는 Golgi 단백이 단백 수송뿐만 아니라 지질 수송에도 중요함을 시사한다. 또한, GRASP55 의 새로운 기능을 밝힘으로써 지방 방울과 연관된 비만, 당뇨, 동맥경화증과 같은 다양한 질환의 병태생리학적 원리와 그에 따른 치료법 개발에 새로운 분자적 기전을 제공하였다는 점에서 의의가 있다.

핵심되는 말: GRASP55, Golgi, 킬로마이크론, 지방 방울, 중성 지방 분해 효소

PUBLICATION LIST

1. He Piao, **Jiyoon Kim**, Shin Hye Noh, Hee-Seok Kweon, Joo Young Kim, Min Goo Lee. Sec16A is critical for both conventional and unconventional secretion of CFTR. *Scientific Reports*. 2017 Jan 9 ; 7: 39887.

2. Won Kyu Kim, SeongJu Yun, Cheol Keun Park, Sebastian Bauer, **Jiyoon Kim**, Min Goo Lee, Hoguen Kim. Sustained mutant KIT activation in the Golgi complex is mediated by PKC-θ in gastrointestinal stromal tumors. *Clinical Cancer Research*. 2016 Dec 28 ; CCR-16-0521.

3. **Jiyoon Kim***, Shin Hye Noh*, He Piao, Dong Hee Kim, Kuglae Kim, Jeong Seok Cha, Woo Young Chung, Hyun-Soo Cho, Joo Young Kim, Min Goo Lee (*co-first author). Monomerization and ER Relocalization of GRASP Is a Requisite for Unconventional Secretion of CFTR. *Traffic*. 2016 Jul ; 17(7):733-53.

4. Jinsei Jung*, **Jiyoon Kim***, Shin Hye Roh, Ikhyun Jun, Robert D. Sampson, Heon Yung Gee, Jae Young Choi, Min Goo Lee (*co-first author). The HSP70 co-chaperone DNAJC14 targets misfolded pendrin for unconventional protein secretion. *Nature Communications*. 2016 Apr 25 ; 7:11386.